# Neural Observer with Lyapunov Stability Guarantee for Uncertain Nonlinear Systems

Song Chen, Tehuan Chen, Chao Xu, and Jian Chu

Abstract—In this paper, we propose a novel nonlinear observer, called the neural observer, for observation tasks of linear time-invariant (LTI) systems and uncertain nonlinear systems by introducing the neural network (NN) into the design of observers. By exploring the method of NN representation to the NN mapping vector, we derive stability analyses (e.g., exponential convergence rate) of LTI and uncertain nonlinear systems that pave the way to solve observation problems using linear matrix inequalities (LMIs) only. Remarkably, the neural observer designed for uncertain systems is based on the ideology of the active disturbance rejection control (ADRC), which can measure the uncertainty in real-time. The LMI results are also significant since we reveal that the observability and controllability of system matrices are required for the existence of solutions of LMIs. Finally, we verify the availability of neural observers on three simulation cases, including the X-29A aircraft model, the nonlinear pendulum, and the four-wheel steering vehicle.

Index Terms— neural network, nonlinear observer, active disturbance rejection control, uncertain systems, linear matrix inequalities, observability and controllability

#### I. INTRODUCTION

ITH the success of machine learning (ML) algorithms on various complex tasks including computer vision and natural language processing, ML meets control theory has been a hot topic in recent years and is attracting more and more researchers. On the one hand, we can use ML to assist in nonlinear control problems, and such data-driven methods can be traced back to neural network (NN) theory [1]–[4]. However, it is not easy to utilize the model information to construct the control input when the model is fragile. Recently, more effective modeling methods based on deep NNs

Manuscript received xx xx, 202x; accepted xx xx, 202x. This work was supported by the National Key Research and Development Program of China under Grant 2019YFB1705800, the National Natural Science Foundation of China number 61973270, the Zhejiang Provincial Natural Science Foundation of China number LY21F030003, and the Zhejiang Provincial Natural Science Foundation of China number LY19A010024. (Corresponding author: Chao Xu.)

S. Chen is with the School of Mathematical Sciences, Zhejiang University, Hangzhou, Zhejiang 310027, China (e-mail: math\_cs@zju.edu.cn).

T. Chen is with School of Mechanical Engineering and Mechanics, Ningbo University, Ningbo, Zhejiang 315211, China, and also with Ningbo Artificial Intelligence Institute, Shanghai Jiao Tong University, Ningbo, Zhejiang 315000, China. (e-mail: chentehuan@nbu.edu.cn).

C. Xu and J. Chu are with the State Key Laboratory of Industrial Control Technology, Institute of Cyber-Systems and Control, Zhejiang University, Hangzhou, Zhejiang 310027, China (e-mail: cxu@zju.edu.cn; chui@iipc.zju.edu.cn).

are gradually coming into our vision. We mention physical-informed ML [5], stable learned deep dynamics [6], and learning nonlinear operators [7]. There are also many works for solving high-dimensional control tasks (e.g., Hamilton-Jacobi-Bellman equation) via deep NNs [8]–[10]. On the other hand, researchers also apply classical control theories to explain why the ML algorithm can work well, including [11]–[14].

Despite many developments in the areas mentioned above, there still exists a major challenge that it is troublesome to directly analyze the control performance (e.g., stability, optimality, etc.) of a system equipped with NN mappings via nonlinear control theory due to various types of nonlinear activation functions and the parameter  $\theta$  in a NN mapping  $\pi_{\theta}(\cdot)$ . This black-box nature makes many deep neural networks are vulnerable to various malicious perturbations [15]. Recently, the work [16], [17] provide an efficient method, composed of the quadratic constraints (QC) and the linear matrix inequality (LMI), to perform the robust stability in equilibrium points of systems controlled by one state-feedback NN mapping controller  $u(k) = \pi_{\theta}(x(k))$ .

In fact, the analysis of robust stability in [16, Theorem. 2] inseparably depends on the assumption that the perturbation  $\Delta$  is bounded and the skilled construction of filter  $\Psi_{\Delta}$ . As for the LMIs conditions that guarantee the stability in [16], [17], they do not explicitly indicate that the existence of solutions of LMIs is true or not. Moreover, the filter  $\Psi_{\Delta}$  may also complicate to solve the LMI condition [16, Theorem. 2]. In our work, instead of constructing the filter  $\Psi_{\Delta}$  for uncertain systems, we inspire by the essential philosophy of the active disturbance rejection control (ADRC) proposed by Han [18] to design neural observers. Moreover, the basic idea of ADRC is to regard the "total uncertainty" as an extended state of the system. Then one can estimate it and finally compensate it in real-time in the control input. Relative theorems about ADRC can be found in [19], [20].

#### A. Paper Contribution

Our contribution can be illustrated by the following aspects: (1) This work falls under the category of using machine learning to achieve control tasks: we introduce a specially structured NN mapping  $\pi_{\theta}(\cdot)$  with a parameter  $\theta$  to design nonlinear neural observers for the observation task in dynamic systems. We first propose two relative definitions: *neural observable* and *neural exponential observable*. Ideologically, for a controllable and observable linear time-invariant (LTI) system, we construct a Luenberger-form neural observer driven

by the feedback of errors and employ the estimated state  $\widehat{x}$  to design the feedback NN control law  $u=\pi_{\theta}(\widehat{x})$ . For two classes of nonlinear systems, high-order nonlinear systems and linear systems with mismatched uncertainties, we respectively design the corresponding neural observers to measure the state and the "total uncertainty" by inheriting the representation of the capacity of NNs [21] and the idea of ADRC [18]. We discuss these details in Sections II and III.

- (2) Then, we first revisit the NN isolation and QCs (see Lemma 1) for one NN mapping  $\pi_{\theta}(\cdot)$ . Next, we show that this method can be extended to deal with a NN mapping vector  $\boldsymbol{\pi}_{\theta}(\cdot)$  composed of K NN mappings, i.e.,  $\boldsymbol{\pi}_{\theta}(\cdot) = [\boldsymbol{\pi}_{\theta_1}^{\top}(\cdot), \cdots, \boldsymbol{\pi}_{\theta_K}^{\top}(\cdot)]^{\top}$  with parameters  $\boldsymbol{\theta} = (\theta_1, \cdots, \theta_K)$ . Moreover, the corresponding QCs for a NN mapping vector are presented in Lemma 2. In addition, we point out that this Lemma can be used to deduce the linear matrix inequality (LMI) of closed-loop dynamics under a feedback interconnection
- (3) The first and the second results (see Theorem 1-2) provide LMI conditions to guarantee the neural exponential observability and globally exponential stability for LTI systems, respectively. Furthermore, in these cases, we reveal the relationship between the existence of solutions for LMIs and the observability and controllability of LTI systems (see Proposition 1-2). Under this fundamental framework, we provide the third and the fourth results (see Theorem 3-4) to achieve the neural observability for high-order nonlinear systems and linear systems with mismatched uncertainties, respectively. Nevertheless, different from Theorem 1-2, Theorem 3-4 can not only guarantee observability but also measure uncertainty in real-time.

This paper is organized as follows. In Section II, we present the keys to the neural observer. In Section III, we propose two definitions of observability and the formulation of neural observers for each class of systems. Moreover, relevant observation problems are also presented. Section IV discusses the NN isolation and QCs method for the NN mapping and the NN mapping vector. Then, the convergence analysis associated with observation problems are provided in Section V. Finally, in Section VI, we provide a detailed set of simulation results to verify the efficiency of our framework, including a linearized aircraft model, a nonlinear inverted pendulum, and a four-wheel steering vehicle.

#### B. Mathematical Notation:

•  $\mathbf{R}^n$  denotes n-dimensional real linear space. In this paragraph, only real linear and finite dimensional spaces are considered. Each space,  $\mathcal{M}$ , possess an inner product  $\langle w,v\rangle = w^\top v$  and a norm  $\|w\|_2^2 = \langle w,w\rangle$ . We use pointwise orders  $\geq$ , > for any vectors  $w,v\in\mathcal{M}$ , i.e.,  $w\geq(>)v\Longleftrightarrow w_i\geq(>)v_i, i\in\{1,\cdots,\dim(\mathcal{M})\}$ . The set of real numbers in the interval  $[a,b]\subset\mathbf{R}$  is  $\mathcal{T}_{[a,b]}$ , and the set of real numbers in the interval  $[a,w)\subset\mathbf{R}$  is  $\mathcal{T}_{\geq a}$ .  $\mathcal{L}(\mathcal{M},\mathcal{N})$  accounts for the space of all linear mappings (matrices) from " $\mathcal{M}$ " to " $\mathcal{N}$ ". For any mappings  $T\in\mathcal{L}(\mathcal{M},\mathcal{N})$ , the induced 2-norm is defined by  $\|T\|_2=\sup_{x\in\mathcal{M},\|x\|_2=1}\|Tx\|_2$ . Specially, when the linear spaces  $\mathcal{M}$  and  $\mathcal{N}$  are identical,  $\mathcal{L}(\mathcal{M},\mathcal{N})$  be abbreviated to

 $\mathcal{L}(\mathcal{M})$ . Given a mapping  $T \in \mathcal{L}(\mathcal{M})$ , i)  $T \succ 0$  represents  $T = T^{\top}$  and  $\langle Tw, w \rangle \geq 0$  for all  $w \in \mathcal{M}$ , where "=" is true if and only if w = 0, and ii)  $\lambda_{\max}(T)$ ,  $\lambda_{\min}(T)$  denote the maximum and minimum eigenvalue, respectively.  $\operatorname{diag}(A_1, \cdots, A_n)$  represents a diagonal block matrix, where the  $i_{th}$  diagonal block is  $A_i$ .  $\mathbf{0}_n, \mathbf{1}_m$  are n-dimensional zero vector and m-dimensional vector whose entries are all ones, respectively.

• The space of k-th continuously differentiable functions from  $\mathcal{M}$  to  $\mathcal{N}$  is denoted by  $C^k(\mathcal{M};\mathcal{N})$ . Similarly, when the spaces  $\mathcal{M}$  and  $\mathcal{N}$  are identical, the notation  $C^k(\mathcal{M})$  is used for short. For any differentiable vector function  $\mathcal{F}(\boldsymbol{x}), \nabla_{\boldsymbol{x}}\mathcal{F}$  is the Jacobi matrix of variable  $\boldsymbol{x} = [x_1, \cdots, x_n]$ , and  $\mathcal{F}_{x_i}$  represents the partial derivative of  $\mathcal{F}$  with respect to  $x_i$ .  $\mathcal{O}(\alpha^k)$  is said to be the infinitesimal of k-order of  $\alpha$  if  $\lim_{\alpha \to 0} \frac{\mathcal{O}(\alpha^k)}{\alpha^k} = c$ ,  $c \neq 0$ .

### II. NEURAL OBSERVER

In this paper, we focus on an underlying, but not necessarily single-input single-output (SISO) or multiple-input multiple-output (MIMO), continuous-time nonlinear and uncertain system formulated by an ordinary differential equation (ODE):

$$\dot{x}(t) = f(x(t), u(t), w(t), t), 
y(t) = Cx(t),$$
(1)

where  $x(t) \in \mathbf{R}^{n_s}$ ,  $u(t) \in \mathbf{R}^{n_u}$ , and  $y(t) \in \mathbf{R}^{n_o}$  denote the state, the control input, and the control output, respectively. Generally, the external disturbances  $w \in \mathbf{R}^{n_d}$  satisfying  $\sup_{t \in \mathcal{T}_{\geq 0}} \|(w, \dot{w})\| < \infty$  are considered in dynamical systems.  $f \in C^1(\mathbf{R}^{n_s} \times \mathbf{R}^{n_u} \times \mathbf{R}^{n_d}; \mathbf{R}^{n_s})$  is a nonlinear functions called the *total uncertainty*, might be partially unknown or totally unknown.  $C \in \mathcal{L}(\mathbf{R}^{n_s}, \mathbf{R}^{n_o})$  denotes the observation matrix of the system.

Due to uncertainties and disturbance, the direct measurement of states would be costly and less credible. Nevertheless, the output measurement is convenient to obtain.

Hence, **Our observation objective** is to design a NN based output-feedback observer (neural observer), such that the state of system (1) is *globally observable* for any initial state x(0) and total uncertainty.

To present the structure of the neural observer, we first introduce an output-feedback neural network (NN) mapping  $\pi_{\theta}(\cdot)$  with a parameter  $\theta$ . We consider  $\pi_{\theta}(\cdot)$  as a feedforward NN with L hidden layers and activation functions  $\sigma(\cdot) \in C(\mathbf{R}|\sigma(0)=0)$  that are identical in all layers. It should be regarded that the input as the  $0_{th}$ -layer and the output as the  $(L+1)_{th}$ -layer, i.e.,  $\pi_{\theta}^{[0]}(x)=x$  and  $\pi_{\theta}^{[L+1]}(x)=\pi_{\theta}(x)$ . Let  $n_l$  be the number of neurons in  $l_{th}$ -layer. By given weights matrix  $W^l \in \mathcal{L}(\mathbf{R}^{n_{l-1}},\mathbf{R}^{n_l})$ , the L-tuple parameter  $\theta$  and the NN mapping  $\pi_{\theta}(\cdot)$  are defined as follows:

$$\theta = (L, n_{\sigma}, W^{1}, \cdots, W^{L+2}), \ n_{\sigma} \triangleq \sum_{i=1}^{L} n_{i}$$

$$\pi_{\theta}^{[l]}(x) = \sigma^{[l]} \left( W^{l} \pi_{\theta}^{[l-1]}(x) \right), \ l = 1, \cdots, L,$$

$$\pi_{\theta}(x) = W^{L+1} \pi_{\theta}^{[L]}(x) + W^{L+2} \pi_{\theta}^{[0]}(x),$$
(2)

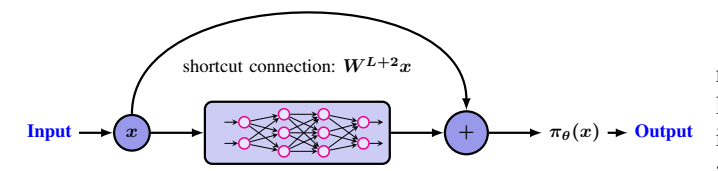


Fig. 1. Residual neural network: a feed-forward NN with  $\boldsymbol{L}$  hidden layers and a shortcut connection.

where  $\sigma^{[l]}(x) = [\sigma(x_1), \cdots, \sigma(x_{n_l})]^{\top}$ . We note that when  $W^{L+2} \neq O$ , the NN mapping is called the residual neural network proposed by He et al. [22] and shown in Fig. 1.

Our work focuses on this novel NN mapping, which facilitates revealing the existence of the parameter  $\theta$  in observer  $\pi_{\theta}(\cdot)$  that would be demonstrated in Remark 5. Based on the defined NN, we construct the neural observer as following:

$$\begin{cases} \hat{x}(t) = g(\hat{x}(t), u(t), \boldsymbol{\pi}_{\boldsymbol{\theta}}(y - \hat{y})), \\ \hat{y} = C\hat{x}, \end{cases}$$
 (3)

where  $\widehat{x} \in \mathbf{R}^{n_{\widehat{s}}}$  and  $\widehat{y} \in \mathbf{R}^{n_o}$  are estimation states and estimation output, respectively.  $\pi_{\boldsymbol{\theta}}(y-\widehat{y}) = [\pi_{\theta_1}^\top (y-\widehat{y}), \cdots, \pi_{\theta_K}^\top (y-\widehat{y})]^\top$  represents the NN mapping vector, where  $\theta_i = (L_i, n_{\sigma_i}, W_i^1, \cdots, W_i^{L_i+2})$ . Moreover, g is a known and continuous function.

#### Remark 1 (The keys to neural observers):

- (1) It is worth noting that the dimension of  $\widehat{x}$  is designed to be no lower than the state x, i.e.,  $n_{\widehat{s}} \geq n_s$ , since the relatively higher dimensional information may improve the effect of the estimate, which is similar to the well-known kernel trick in machine learning algorithms (like Gaussian process regression [23]).
- (2) Furthermore, the construction of the continuous function *g* need to acquire some transparent knowledge from the structure of system (1), such as model order, modeled linear dynamics, and so on.
- (3) Moreover, in the part of NNs in a neural observer, to trade-off the computational complexity and estimation accuracy, we could take some parameters in  $\pi_{\theta}$  to be identical, such as  $\theta_{n_i} = \theta_{n_j}$  for  $i, j \in I$ , where I is an index-subset of  $\{1, \cdots, K\}$ .
- (4) And we leverage the representation of the capacity of NNs [21] for uncertainties to compensate the estimation tasks.

The block diagram of the neural observation framework is shown in Fig. 2.

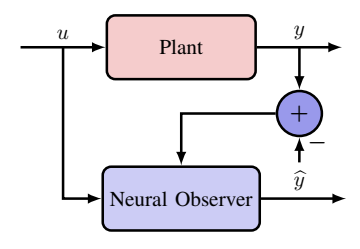


Fig. 2. The block diagram of the neural observation framework: the observed error  $y(t) - \hat{y}(t)$  is the input of NN mapping vector in the neural observer.

#### III. PROBLEM FORMULATION

Before presenting the main results, we first state the three main problems we will consider in this work: how to design reliable neural observers structure for observation tasks. Specifically, we hope to find a family of NN  $\pi_{\theta}$  and  $g(\widehat{x}, u, \pi_{\theta})$  architectures for output-feedback observation of three classes of systems (1). Furthermore, this architecture must further ensure the existence of parameter  $\theta$  to enable the implemented neural observer for observation objectives.

Formally, we have the following definition of neural observers:

**Definition 1 (neural observable):** Suppose that there exist the NN mapping vector  $\pi_{\theta}$  such that the closed-loop system composed of (1) and (3) satisfies for all x(0),  $\hat{x}(0)$ ,

 $||x(t) - T\hat{x}(t)||_2 \to 0$ , in some sense, for example,  $t \to +\infty$ ,

where  $T \in \mathcal{L}(\mathbf{R}^{n_{\widehat{s}}}, \mathbf{R}^{n_s})$  with  $T_{ij} = 1, i = j; T_{ij} = 0, else$ . Then we say that the system (1) is **neural observable**.

Note that T = I if  $n_s$  is equal to  $n_{\widehat{s}}$ . And T is also applied in the following definition.

**Definition 2 (neural exponential observable):** Consider the aforementioned closed-loop system. If there exist two constants  $M>0,\ \kappa>0$ , and the NN mapping vector  $\pi_{\theta}$  such that for any initial states x(0) and  $\widehat{x}(0)$ , the closed-loop system satisfies that for all t>0,

$$||x(t) - T\widehat{x}(t)||_2 \le M \exp^{-\kappa t} \{||x(0)||_2 + ||\widehat{x}(0)||_2\},$$

then the system (1) is said to be **neural exponential observable**.

Next, based on the above definitions, we introduce three canonical observation problems: under what conditions are linear systems without uncertainties, high-order systems, or linear systems involving mismatched uncertainties neural (exponential) observable?

# A. Neural Observers for Linear Systems

As a primary step, we consider the following continuoustime LTI system without uncertainties that is still one case in (1)

$$\begin{cases} \dot{x} = Ax + Bu, \\ y = Cx, \end{cases} \tag{4}$$

where  $A \in \mathcal{L}(\mathbf{R}^{n_s})$  and  $B \in \mathcal{L}(\mathbf{R}^{n_s}, \mathbf{R}^{n_u})$  are known system matrices. For the neural observable problem, we take the standard assumption.

**Assumption 1:** (A, B) is controllable, and (C, A) is observable.

Due to the availability of system matrices (A, B, C), we can construct an underlying neural observer corresponding to (4), which is consistent with Remark 1, as follows:

$$\begin{cases} \dot{\widehat{x}} = A\widehat{x} + Bu + \pi_{\theta_1}(y - \widehat{y}), \\ \widehat{y} = C\widehat{x}, \end{cases}$$
 (5)

where  $\pi_{\theta_1}(\cdot)$  is a NN mapping with a single parameter  $\theta_1$ . The concrete neural observation diagram for the system (4) can be shown in Fig. 3. Hence, we informally list the following intuitive questions:

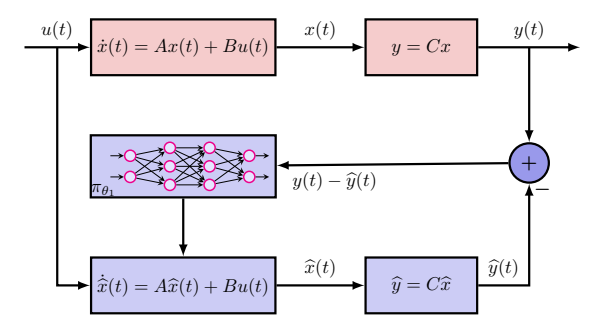


Fig. 3. The diagram of neural observers for LTI (continuous) systems

**Problem 1.1:** Under Assumption 1, what is the necessary condition for the system (4) to be neural exponential observable?

We remark that in analogy with classical control if the system (4) is neural exponential observable, the estimation states  $\hat{x}(t)$  can be utilized to model the feedback controller for system (4). By the inspiration from NN controllers for discrete-time LTI systems in [16], [17], we construct the following observer-based NN controller:

$$u(t) = \pi_{\theta_2}(\widehat{x}). \tag{6}$$

Consequently, we informally raise another question for system (4) as follows:

**Problem 1.2:** By applying the control law  $u(t) = \pi_{\theta_2}(\widehat{x})$ , the problem is to find a suitable NN mapping  $\pi_{\theta_2}(\cdot)$  such that  $\lim_{t\to\infty} \|x(t)\|_2 = 0$ , meanwhile system (4) is neural exponential observable under the given Assumption 1.

Without the demonstration, we call that the results of the above questions are the most basic ones, which could serve in the following sections.

#### B. Neural Observers for High-order Nonlinear Systems

Consider a class of SISO uncertain systems, described by the following differential equation with an order of n:

$$\begin{cases} x^{(n)}(t) = \mathcal{F}(t, x(t), \dots, x^{(n-1)}(t), w(t)) + bu(t), \\ y(t) = x(t), \end{cases}$$
 (7)

where  $\mathcal{F}(\cdot)$  is an unknown and continuously differentiable function, and b is a known constant. The above system (7) is an integral-chain system that can be rewritten as follows:

$$\begin{cases} \dot{\boldsymbol{x}} = \mathcal{A}\boldsymbol{x} + L(t, \boldsymbol{x}, w, u), \\ y = c\boldsymbol{x}, \end{cases}$$
 (8)

where  $\boldsymbol{x} = [x_1, \cdots, x_n]^{\top}$ ,  $\boldsymbol{\mathcal{A}} = (a_{ij})_{n \times n}$  is defined by

$$a_{ij} = \begin{cases} 1, & i+1=j \\ 0, & else \end{cases}, c = [1, 0, \dots, 0],$$
  
 $L(t, x, w, u) = [0, \dots, 0, \mathcal{F}(t, \boldsymbol{x}, w) + bu]^{\top}$ 

We remark that as the order n=2, the systems (7) can describe basic systems via Newton's second law, including the inverted pendulum model and so on. And due to the differentiability of  $\mathcal{F}(\cdot)$ , the system (8) is a case of (1). Then, we make some basic assumptions for nonlinear systems (7).

**Assumption 2:** (1) Firstly, there exists a continuous function  $\chi(x,w)$  such that  $\sup_{t\in\mathcal{T}_{>0}}\|(\mathcal{F},\nabla\mathcal{F})\|_2\leq \chi(x,w)$ .

(2) Secondly, there exists a bounded control u(t) such that  $\sup_{t \in \mathcal{T}_{\geq 0}} \{ \| \boldsymbol{x}(t) \|_2 + |u(t)| \} < \infty.$ 

From the Remark 1, we can regard the matrix A and c as the knowledge that is used to describe the corresponding neural observer for systems (7):

$$\begin{cases}
\dot{\hat{x}}_i = \hat{x}_{i+1} + \epsilon^{n-i} \pi_{\theta_i} (\epsilon^{-n} (y - \hat{y})), & i = 1, \dots, n, \\
\dot{\hat{x}}_{n+1} = \epsilon^{-1} \pi_{\theta_{n+1}} (\epsilon^{-n} (y - \hat{y})) + bu, \\
\hat{y} = c\hat{x},
\end{cases} \tag{9}$$

where  $\epsilon$  is a positive constant,  $\widehat{x} = [\widehat{x}_1, \cdots, \widehat{x}_n]^{\top}$ . Based on the neural observer, we note that the simplest way to satisfy Assumption 2 is to design the bounded control in the linear form  $u(t) = \frac{\rho \sum_{i=1}^n k_i \operatorname{sat}_{M_i}(\rho^{n-i}\widehat{x}_i(t)) - \operatorname{sat}_{M_{n+1}}(\widehat{x}_{n+1}(t))}{b}$  with parameters of  $\rho, k_i, M_i$ , where the control gain  $K = [k_1, \cdots, k_n]$  is designed by  $A + c_0 K$  is Hurwitz with  $c_0 = [0, \cdots, 1]^{\top}$ . The details of which can be found in [24].

Therefore, we informally introduce the observation problem for systems (7):

**Problem 2.1:** Consider the neural observer-based closed system (7), (9). Under the Assumption 2, we need to investigate the necessary conditions for the underlying result:

• the system (7) is neural observable;

Remark 2: We need to point out that the formulation of the neural observer (9) resembles the extended state observer (ESO) in active disturbance rejection control [25], [26]. But in fact, the construction of nonlinear functions in ESO is complicated in industrial processes. Hence, due to the approximating capability of NNs, we can take advantage of this property to relieve these pressures.

# C. Neural Observers for Linear Systems with Mismatched Uncertainties

Finally, the following MIMO linear system with mismatched uncertainties is taken into account, which is another case of systems (1).

$$\begin{cases} \dot{x} = Ax + Bu + \mathcal{K}(x, w, t), \\ y = Cx, \end{cases}$$
 (10)

where A and B are defined the same way as (4).  $\mathcal{K}(\cdot)$  represents the uncertainty associated with x(t), w(t), and t.

**Remark 3:** Since the system (7) is an affine control system, the system (7) is one case of (10). Thus, we know that (10) is not restricted to the integral chain form [27], but attaches a more generality compared with (7).

**Assumption 3:** • C is invertible such that  $(\mathbf{C}, \mathbf{I})$  is observable, where  $\mathbf{C} = [C, O]$ , and  $\mathbf{I} = \begin{bmatrix} O & I \\ O & O \end{bmatrix}$  with  $I \in \mathcal{L}(\mathbf{R}^{n_s})$ ;

- $\sup_{t\in\mathcal{T}_{\geq 0}}(\|\mathcal{K}\|_2,\|\nabla\mathcal{K}\|_2)\leq \varpi(x,w)$ , where  $\varpi(x,w)\in C(\mathbf{R}^{n_s+1};\mathbf{R})$
- there exists a output-feedback control law u=u(y) such that the state x(t) is bounded.

By the principle shown in Remark 1, we serve (A, B, C) as the knowledge to design the neural observer, as shown below:

$$\begin{cases}
\dot{\widehat{x}}_1 = \widehat{x}_2 + A\widehat{x}_1 + Bu + \pi_{\theta_1}(\epsilon^{-1}(y - \widehat{y})), \\
\dot{\widehat{x}}_2 = \epsilon^{-1}\pi_{\theta_2}(\epsilon^{-1}(y - \widehat{y})), \\
\widehat{y} = \mathbf{C}\widehat{x},
\end{cases} (11)$$

where  $\epsilon$  is positive,  $\hat{x} = [\hat{x}_1^\top, \hat{x}_2^\top]^\top$ . In the end, a problem is raised accordingly:

**Problem 3.1:** We need to seek out the necessary condition for system (10) to be neural observable under Assumption 3

### IV. NN REPRESENTATION AND NN MAPPING VECTOR

We will present the main theorems of this work in a later section: Theorems 1-4, which directly solve each of the problems mentioned above. As a necessary prelude, however, we introduce the following two definitions. The first definition is about the isolation of nonlinear activation function from the linear operation of NNs defined in (2) and QCs for activation functions, similarly done in [16], [28] and [29], respectively. In the second, we define the concept of NN mapping vector and QCs for NN mapping vector.

# A. NN Isolation and QCs for Single NN mapping

For a specific NN mapping  $\pi_{\theta}$  and the input  $x \in \mathbf{R}^{\text{Input}}$ , we define  $w^0 = x$  and  $\xi^i = W^i w^{i-1}$ ,  $w^i = \sigma^{[i]}(\xi^i)$ , i = $1, \dots, L$ . By collecting the input and output of all activation functions, we denote two  $n_{\sigma}$  dimensional vectors  $\xi_{\sigma}$  and  $w_{\sigma}$ as follows:

$$\xi_{\sigma} \triangleq \left[ \begin{array}{c} \xi^{1} \\ \vdots \\ \xi^{L} \end{array} \right], \ w_{\sigma} \triangleq \left[ \begin{array}{c} w^{1} \\ \vdots \\ w^{L} \end{array} \right].$$

Then, by recalling that  $\pi_{\theta}(x) = W^{L+1}w^L + W^{L+2}\pi_{\theta}^{[0]}(x)$ and  $\pi_{\theta}^{[0]}(x) = x$ , the NN mapping  $\pi_{\theta}$  can be rewritten into

$$\begin{bmatrix} \pi_{\theta} \\ \xi^1 \\ \vdots \\ \xi^L \end{bmatrix} = \begin{bmatrix} W^{L+2} & O & O & \cdots & W^{L+1} \\ \hline W^1 & O & \cdots & O & O \\ O & W^2 & \cdots & O & O \\ \vdots & \vdots & \ddots & \vdots & \vdots \\ O & O & \cdots & W^L & O \end{bmatrix} \begin{bmatrix} x \\ w^1 \\ \vdots \\ w^L \end{bmatrix}, \text{ a single layer, with no shortcut connection } (W^{L+2} = O), \text{ and } use the fal}(s, \gamma, \delta) \text{ function as the activation function, in this sense, then the extended state observers with the fal}(s, \gamma, \delta)$$
 function can be included in neural observers.

which can be abbreviated in the following formulation:

$$\begin{bmatrix} \pi_{\theta}(x) \\ \xi_{\sigma} \end{bmatrix} = \begin{bmatrix} N_{\pi x} & N_{\pi w} \\ N_{\xi x} & N_{\xi w} \end{bmatrix} \begin{bmatrix} x \\ w_{\sigma} \end{bmatrix}$$
 (13)

Now, we define two following linear mappings:

$$R_{\pi} \triangleq \begin{bmatrix} I & O \\ N_{\pi x} & N_{\pi w} \end{bmatrix}, \quad R_{\xi} \triangleq \begin{bmatrix} N_{\xi x} & N_{\xi w} \\ O & I \end{bmatrix}, \quad (14)$$

then derive the corresponding linear transformations for  $[x^{\top}, w_{\sigma}^{\top}]^{\top}$ :

$$\left[\begin{array}{c} x \\ \pi_{\theta}(x) \end{array}\right] = R_{\pi} \left[\begin{array}{c} x \\ w_{\sigma} \end{array}\right], \quad \left[\begin{array}{c} \xi_{\sigma} \\ w_{\sigma} \end{array}\right] = R_{\xi} \left[\begin{array}{c} x \\ w_{\sigma} \end{array}\right].$$

To avoid confusion, we must emphasize that two identical matrices I in  $R_{\pi}$  and  $R_{\xi}$  belong to different spaces of linear mappings,  $\mathcal{L}(\mathbf{R}^{\text{Input}})$  and  $\mathcal{L}(\mathbf{R}^{n_{\sigma}})$ , respectively.

**Remark 4:** Due to the existence of a shortcut connection shown in Fig. 1, the matrix  $N_{\pi x}$  in (14) is a not zero matrix that makes a difference with [16]. However, in addition, nonzero matrix  $N_{\pi x}$  plays a crucial role in neural observability, which would be certified in Proposition 1.

Next, we deal with another thorny difficulty in analyzing NNs, which is the composition of nonlinear activation functions. The key is to remove the non-linearity of activation functions but retain some linear properties derived from geometry.

Consider the activation function  $\sigma(\cdot) \in C(\mathbf{R}|\sigma(0) = 0)$ . Then, the function is said to be sector bounded in sector  $[\alpha, \beta]$ with  $\alpha \leq \beta < \infty$  if the following inequality holds for all  $s \in \mathbf{R}$ :

$$(\sigma(s) - \alpha s)(\beta s - \sigma(s)) > 0.$$

Intuitively, the above inequality implies that the function y = $\sigma(s)$  lies in the open region of  $y = \alpha s$ ,  $y = \beta s$ , and the origin. For the sector bounded, as mentioned earlier, the nonlinear functions commonly used in practice [26] are of the following

$$fal(s, \gamma, \delta) = \begin{cases} |s|^{\gamma} \operatorname{sgn}(s), |s| > \delta, \\ \frac{s}{\delta^{1-\gamma}}, |s| \le \delta, \end{cases}$$

which also satisfies the sector boundedness illustrated in Fig. 4. In other words, when we take the NN in the neural observer as

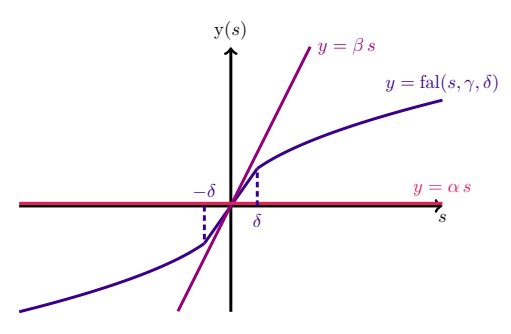


Fig. 4. Sector boundedness for  $\operatorname{fal}(s,\gamma,\delta)$ : The function  $\operatorname{fal}(s,\gamma,\delta)$  is sector bound in sector  $[\alpha,\beta]$ , in which we set  $\alpha=0$  and  $\beta\geq \delta^{\gamma-1}$ .

function can be included in neural observers.

Next, the activation functions  $\sigma(\cdot)$  at each hidden layer are sector bounded in sector  $[\alpha_i, \beta_i], i = 1, \dots, n_{\sigma}$ , respectively. By denoting sector vectors  $\alpha_{\sigma} = [\alpha_1, \cdots, \alpha_{n_{\sigma}}]$  and  $\beta_{\sigma} =$  $[\beta_1, \cdots, \beta_{n_\sigma}]$ , the QCs for one NN mapping are provided as

**Lemma 1** ( [16]): Let  $\alpha_{\sigma}, \beta_{\sigma} \in \mathbf{R}^{n_{\sigma}}$  are defined above with  $\alpha_{n_{\sigma}} \leq \beta_{n_{\sigma}}$ . If  $\lambda_{\sigma} \in \mathbf{R}^{n_{\sigma}}$  and  $\lambda_{\sigma} \geq \mathbf{0}_{n_{\sigma}}$ , then:

$$\begin{bmatrix} \xi_{\sigma} \\ w_{\sigma} \end{bmatrix}^{\top} \Psi_{\sigma}^{\top} M_{\sigma}(\lambda_{\sigma}) \Psi_{\sigma} \begin{bmatrix} \xi_{\sigma} \\ w_{\sigma} \end{bmatrix} \ge 0$$

where  $\mathbf{0}_{\sigma}$  is a zero vector,

$$\Psi_{\sigma} \triangleq \begin{bmatrix} \operatorname{diag}(\beta_{\sigma}) & -I \\ -\operatorname{diag}(\alpha_{\sigma}) & I \end{bmatrix}, \\
M_{\sigma}(\lambda_{\sigma}) \triangleq \begin{bmatrix} O & \operatorname{diag}(\lambda_{\sigma}) \\ \operatorname{diag}(\lambda_{\sigma}) & O \end{bmatrix}$$
(15)

# B. NN Isolation and QCs for NN mapping vector

Whereafter, we try to isolate the non-linearity of NN mapping vector  $\boldsymbol{\pi}_{\boldsymbol{\theta}}(x) = [\boldsymbol{\pi}_{\theta_1}^\top(x), \cdots, \boldsymbol{\pi}_{\theta_K}^\top(x)]^\top$  shown in Fig. 5, which consists of K NN mappings with different parameters  $\boldsymbol{\theta}_i$ .

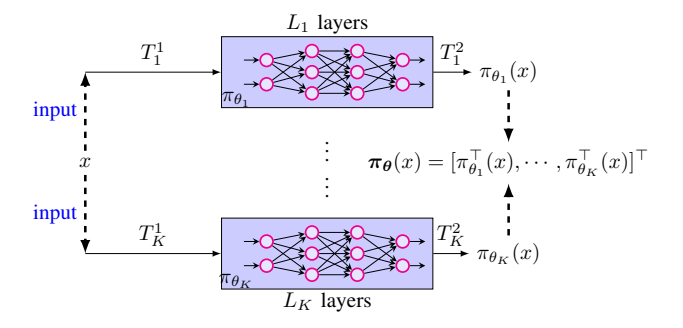


Fig. 5. The diagram of NN mapping vector

Denote  $w_k^0=x$  and  $\xi_k^i=W_k^iw_k^{i-1},~w_k^i=\sigma^{[i]}(\xi_k^i),~i=1,\cdots,L_k,~k=1,\cdots,K,$  and two  $n_{\sigma_k}\triangleq\sum_{i=1}^{L_k}n_i$  dimensional vectors  $\xi_{\sigma_k}$  and  $w_{\sigma_k}$  as follows:

$$\xi_{\sigma_k} \triangleq \begin{bmatrix} \xi_k^1 \\ \vdots \\ \xi_k^{L_k} \end{bmatrix}, \ w_{\sigma_k} \triangleq \begin{bmatrix} w_k^1 \\ \vdots \\ w_k^{L_k} \end{bmatrix}.$$

With the help of (13), we derive the following transformation

$$\left[ \begin{array}{c} \pi_{\theta_k}(x) \\ \xi_{\sigma_k} \end{array} \right] = \underbrace{ \left[ \begin{array}{cc} N_{\pi_k x} & N_{\pi_k w_k} \\ N_{\xi_k x} & N_{\xi_k w_k} \end{array} \right] }_{N_k} \left[ \begin{array}{c} x \\ w_{\sigma_k} \end{array} \right],$$

$$N_k = \begin{bmatrix} T_k^2 W_k^{L_k + 2} T_k^1 & O & O & \cdots & T_k^2 W_k^{L_k + 1} \\ \hline W_k^1 T_k^1 & O & \cdots & O & O \\ O & W_k^2 & \cdots & O & O \\ \vdots & \vdots & \ddots & \vdots & \vdots \\ O & O & \cdots & W_k^{L_k} & O \end{bmatrix}.$$

We suppose  $\xi_{\sigma}^K = [\xi_{\sigma_1}^{\top}, \cdots, \xi_{\sigma_K}^{\top}]^{\top}$  and  $w_{\sigma}^K = [w_{\sigma_1}^{\top}, \cdots, w_{\sigma_K}^{\top}]^{\top}$  and have

$$\begin{bmatrix} \boldsymbol{\pi}_{\boldsymbol{\theta}}(x) \\ \boldsymbol{\xi}_{K}^{K} \end{bmatrix} = \begin{bmatrix} \widehat{N}_{\boldsymbol{\pi}x} & \widehat{N}_{\boldsymbol{\pi}w} \\ \widehat{N}_{\boldsymbol{\xi}x} & \widehat{N}_{\boldsymbol{\xi}w} \end{bmatrix} \begin{bmatrix} x \\ w_{\sigma}^{K} \end{bmatrix}, \quad (16)$$

where the block matrices equal to

$$\widehat{N_{\pi x}} = \begin{bmatrix} N_{\pi_1 x} \\ \vdots \\ N_{\pi_K x} \end{bmatrix}, \ \widehat{N_{\pi w}} = \operatorname{diag}(N_{\pi_1 w_1}, \cdots, N_{\pi_K w_K}),$$

$$\widehat{N_{\xi x}} = \begin{bmatrix} N_{\xi_1 x} \\ \vdots \\ N_{\xi_K x} \end{bmatrix}, \ \widehat{N_{\xi w}} = \operatorname{diag}(N_{\xi_1 w_1}, \cdots, N_{\xi_K w_K}).$$

Then, it is easy to verify that the following transformations derived from (16) are held on:

$$\begin{bmatrix} x \\ \pi_{\theta}(x) \end{bmatrix} = \widehat{R_{\pi}} \begin{bmatrix} x \\ w_{\sigma}^{K} \end{bmatrix}, \quad \begin{bmatrix} \xi_{\sigma}^{K} \\ w_{\sigma}^{K} \end{bmatrix} = \widehat{R_{\xi}} \begin{bmatrix} x \\ w_{\sigma}^{K} \end{bmatrix},$$

where

$$\widehat{R}_{\pi} \triangleq \left[ \begin{array}{cc} I & O \\ \widehat{N}_{\pi x} & \widehat{N}_{\pi w} \end{array} \right], \quad \widehat{R}_{\xi} \triangleq \left[ \begin{array}{cc} \widehat{N}_{\xi x} & \widehat{N}_{\xi w} \\ O & I \end{array} \right]. \quad (17)$$

Afterward, by gathering each sector vector  $\alpha_{\sigma_k}$ ,  $\beta_{\sigma_k}$  from  $\pi_{\theta_k}(x)$  and making  $n_{\sigma}^K = \sum_{k=1}^K n_{\sigma_k}$ ,  $\alpha_{\sigma}^K = [\alpha_{\sigma_1}^\top, \cdots, \alpha_{\sigma_K}^\top]^\top$ ,  $\beta_{\sigma}^K = [\beta_{\sigma_1}^\top, \cdots, \beta_{\sigma_K}^\top]^\top$ , we take a vector  $\lambda_{\sigma}^K \in \mathbf{R}^{n_{\sigma}^K}$  with positive components and the following matrices with the parameter K

$$\Psi_{\sigma}(\boldsymbol{\alpha}, \boldsymbol{\beta}; K) \triangleq \begin{bmatrix} \operatorname{diag} \left( \beta_{\sigma}^{K} \right) & -I \\ -\operatorname{diag} \left( \alpha_{\sigma}^{K} \right) & I \end{bmatrix}, \\
\mathbf{M}_{\sigma}(\lambda_{\sigma}^{K}; K) \triangleq \begin{bmatrix} O & \operatorname{diag}(\lambda_{\sigma}^{K}) \\ \operatorname{diag}(\lambda_{\sigma}^{K}) & O \end{bmatrix}.$$
(18)

Then, it suffices to show the following QC for NN mapping vector:

**Lemma 2** (K **Law of Quadratic Constraint):** For any  $\lambda_{\sigma}^{K} \geq \mathbf{0}_{n_{\sigma}^{K}}$ ,  $\xi_{\sigma}^{K}$  and  $w_{\sigma}^{K}$  defined in (16), matrices  $\Psi_{\sigma}(\alpha, \beta; K)$  and  $\mathbf{M}_{\sigma}(\lambda_{\sigma}^{K}; K)$  (simply denoted as  $\Psi(K)$  and  $\mathbf{M}(K)$ ) defined in (18), the QC is held for NN mapping vector  $\boldsymbol{\pi}_{\theta}$  consisting of K NN mappings

$$\begin{bmatrix} \xi_{\sigma}^{K} \\ w_{\sigma}^{K} \end{bmatrix}^{\top} \mathbf{\Psi}(K)^{\top} \mathbf{M}(K) \mathbf{\Psi}(K) \begin{bmatrix} \xi_{\sigma}^{K} \\ w_{\sigma}^{K} \end{bmatrix} \ge 0$$

*Proof:* The proof is given in Appendix I.

Notice that as K=1, Lemma 1 is a case of Lemma 2. In the relevant sections below, we would pre-state the value of the parameter K and the input x for NN mapping vector.

#### V. MAIN RESULT

The approach in the previous section can be summarized as follows: by using isolation of non-linearity for a NN mapping and QCs for activation functions, we extend the characterization of a single NN mapping to NN mapping vector composed of several NN mappings. In this section, we utilize this approach to answer the questions proposed in Section III.

### A. Neural Observers for Systems without Uncertainty

For the intuitiveness and simplicity of the arguments, we start analyzing of the neural observability of linear systems. First, we formally state our main result for Problem 1.1 in the following theorem.

**Theorem 1:** Consider a NN mapping  $\pi_{\theta}$  with parameter  $\theta$  and a vector  $\lambda_{\sigma}$  that satisfies the quadratic constraint in Lemma 1. We update  $W^{L+2}$  and  $W^1$  in (14) to  $W^{L+2}C$  and  $W^1C$ , respectively. If there exists a matrix  $P \in \mathcal{L}(\mathbf{R}^{n_s})$  and  $P \succ O$  such that

$$R_{\pi}^{\top} \begin{bmatrix} A^{\top}P + PA & P \\ P & O \end{bmatrix} R_{\pi} + R_{\xi}^{\top}\Psi_{\sigma}^{\top}M_{\sigma}(\lambda_{\sigma})\Psi_{\sigma}R_{\xi} \prec O,$$
(19)

then the LTI system (4) is neural exponential observable, equivalently,

$$||x(t) - \widehat{x}(t)||_2 \le M \exp^{-\kappa t} \{||x(0)||_2 + ||\widehat{x}(0)||_2\},$$

where  $R_{\pi}$ ,  $R_{\xi}$ , and  $\Psi_{\sigma}$ ,  $M_{\sigma}(\lambda_{\sigma})$  are defined in (14), and (15), respectively.

*Proof:* First, we suppose that the existence of the matrix P is true. Denote  $e(t) = \widehat{x}(t) - x(t)$ , then from (4) and (5), it is not difficult to obtain

$$\begin{cases} \dot{e}(t) = Ae(t) + v(t), \\ v(t) = \pi_{\theta}(Ce(t)). \end{cases}$$

Equivalently, the form of input of  $\pi_{\theta}$  can be regarded as e(t) by updating  $W^{L+2}$  and  $W^1$  in (14) to  $W^{L+2}C$  and  $W^1C$ , respectively. Recall that  $P \succ O$ , we define a radially unbounded Lyapunov function  $V: \mathbf{R}^{n_s} \to \mathbf{R}, \ e(t) \mapsto e^\top(t) Pe(t)$ . Then, the time derivative of V along the trajectories of e(t) is given by

where  $\star$  can be inferred from symmetry. By using the transformation from (14) and the strict LMI (19), we imply that there exists  $\epsilon>0$  such that the left/right multiplication of the LMI by  $\left[e^{\top},w_{\sigma}^{\top}\right]$  and its transpose yields

$$\begin{split} & [\star]^\top \left[ \begin{array}{cc} A^\top P + PA & P \\ P & O \end{array} \right] \left[ \begin{array}{c} e(t) \\ v(t) \end{array} \right] \\ & + [\star]^\top \Psi_\sigma^\top M_\sigma(\lambda_\sigma) \Psi_\sigma \left[ \begin{array}{c} \xi_\sigma(t) \\ w_\sigma(t) \end{array} \right] \leq -\epsilon (\|e(t)\|_2^2 + \|v(t)\|_2^2). \end{split}$$

Therefore, by using Gronwall-Bellman inequality <sup>1</sup>, we deduce that  $\frac{dV}{dt}\Big|_{e(t)} \le -\epsilon \|e(t)\|_2^2 \le -\frac{\epsilon V(e(t))}{\lambda_{\max}(P)}$ , which in turn gives

$$\begin{split} \lambda_{\min}(P) \|e(t)\|_2^2 &\leq V(e(t)) \leq e^{-\frac{\epsilon t}{\lambda_{\max}(P)}} V(e(0)) \\ &\leq \lambda_{\max}(P) e^{-\frac{\epsilon t}{\lambda_{\max}(P)}} \|e(0)\|_2^2. \end{split}$$

As a consequence, we obtain

$$||x(t) - \widehat{x}(t)||_{2} \leq \sqrt{\lambda_{\max}(P)/\lambda_{\min}(P)} e^{-\frac{\epsilon t}{2\lambda_{\max}(P)}} ||e(0)||_{2},$$
  
$$\leq Me^{-\frac{\epsilon t}{2\lambda_{\max}(P)}} \{||x(0)||_{2} + ||\widehat{x}(0)||_{2}\}.$$

This completes the proof of Theorem 1.

Furthermore, it is not difficult to imply that the neural exponential observability of system (4) and the existence of  $\theta$  in  $\pi_{\theta}$  depend heavily on the existence of P, i.e., the solution of LMI (19). Hence, a natural sub-question is: Under what conditions does the solution P in LMI exist? To our best knowledge, this question has not been effectively solved in the NN-based closed-loop control (for example, [16, Theorem 1] and [17, Theorem 1]) at present. Therefore, we present the following proposition to answer this sub-question.

**Proposition 1:** We set 
$$\alpha_{\sigma} = \mathbf{0}_{n_{\sigma}}$$
,  $\widetilde{A} = A + N_{\pi x}$  with

Consider  $u(t) \in C^1(\mathcal{T}_{\geq 0})$  and Lemma 1, c(t) and f(t) are continuous functions defined in  $t \in \mathcal{T}_{\geq 0}$ . If  $\dot{u} \leq c(t)u(t) + f(t)$  for all  $t \in \mathcal{T}_{\geq 0}$ , then we have  $u(t) \leq u(0)e^{\int_0^t c(\rho)d\rho} + \int_0^t f(s)e^{\int_s^t c(\rho)d\rho} ds, t \in \mathcal{T}_{\geq 0}$ .

 $N_{\pi x}=W^{L+2}C,\ Q\in\mathcal{L}(\mathbf{R}^{n_s})$  is a diagonal matrix with positive diagonal entries, and  $P=\int_0^\infty e^{\widetilde{A}^{\mathsf{T}}t}Qe^{\widetilde{A}t}dt$ . Suppose that there exists  $\lambda_\sigma>\mathbf{0}_{n_\sigma}$  such that

- (i)  $||M_1||_{\infty} \leq \min_i(q_i)$ , where  $M_1 = -PN_{\pi w} N_{\xi x}^{\top} R_1$  with  $R_1 = \operatorname{diag}(\lambda_{\sigma} \circ \beta_{\sigma})^2$ , and  $q_i$  is the  $i_{th}$  diagonal entry in Q,
- (ii)  $\|M_1^{\top}\|_{\infty} + \|M_2\|_{\infty} \leq 2 \min_i(\lambda_{\sigma,i})$ , where  $\lambda_{\sigma,i}$  is the  $i_{th}$  element of  $\lambda_{\sigma}$ ,  $M_2 = R_1 N_{\xi w} + N_{\xi w}^{\top} R_1$ .

Then LMI (19) has a solution P if and only if (C, A) is observable.

*Proof:* First, we unfold and directly compute the matrices in left side in LMI (19) as follows:

$$R_{\pi}^{\top} \begin{bmatrix} A^{\top}P + PA & P \\ P & O \end{bmatrix} R_{\pi} = \begin{bmatrix} \widetilde{A}^{\top}P + P\widetilde{A} & PN_{\pi w} \\ \star & O \end{bmatrix},$$

$$R_{\xi}^{\top}\Psi_{\sigma}^{\top}M_{\sigma}(\lambda_{\sigma})\Psi_{\sigma}R_{\xi} = \begin{bmatrix} O & N_{\xi x}^{\top}R_{1} \\ \star & -2\operatorname{diag}(\lambda_{\sigma}) \end{bmatrix}.$$

To prove the Proposition 1, we need the following steps.

**Step 1**: A strictly diagonally dominant diagonal matrix  $T = (t_{ij}) \in \mathcal{L}(\mathbf{R}^m)$  has positive diagonal entries, which means that for all  $i = 1, \dots, m$ , we have  $|t_{ii}| > \Sigma_{i \neq j} |t_{ij}|$  and  $t_{ii} > 0$ . Then, this matrix is positively definite. Specifically, for all  $x \in \mathbf{R}^m$ ,

$$x^{\top} T x = \sum_{i=1}^{m} t_{ii} x_{i}^{2} + \sum_{i \neq j} t_{ij} x_{i} x_{j},$$

$$> \sum_{i=1}^{m} \left( \sum_{i \neq j} |t_{ij}| \right) x_{i}^{2} - \sum_{i \neq j} |t_{ij}| |x_{i}| |x_{j}|,$$

$$= \sum_{j>i} \left( |t_{ij}| \left( x_{i}^{2} + x_{j}^{2} - 2 |x_{i}| |x_{j}| \right) \right) \ge 0.$$

Step 2:  $\Rightarrow$  For the sufficiency, due to the observability of (C,A), then  $\widetilde{A}=A+N_{\pi x}$  is a Hurwitz matrix by taking the matrix  $W^{L+2}$  in  $N_{\pi x}=W^{L+2}C$  is a pole assignment matrix for  $\widetilde{A}$ . Since  $\widetilde{A}=A+N_{\pi x}$  is a Hurwitz matrix, we imply that the Lyapunov equation  $-(\widetilde{A}^\top P+P\widetilde{A})=Q$  has a unique solution  $P=\int_0^\infty e^{\widetilde{A}^\top t}Qe^{\widetilde{A}t}dt$  that is finite, i.e.,  $\|P\|_F<\infty$ . Therefore, we can rewrite the LMI into

$$R_{\pi}^{\top} \begin{bmatrix} A^{\top}P + PA & P \\ P & O \end{bmatrix} R_{\pi} + R_{\xi}^{\top} \Psi_{\sigma}^{\top} M_{\sigma}(\lambda_{\sigma}) \Psi_{\sigma} R_{\xi}$$
$$= -\underbrace{\begin{bmatrix} Q & M_{1} \\ M_{1}^{\top} & 2 \operatorname{diag}(\lambda_{\sigma}) - M_{2} \end{bmatrix}}_{\triangleq M_{0}}.$$

By substituting  $N_{\xi w}$  into  $M_2$  from above, we can show that  $M_2$  is a symmetric matrix with zero diagonal entries. Hence, under the assumptions (i) and (ii), the LMI (19) is satisfied due to  $M_0$  is strictly diagonally dominant.

 $\Leftarrow$  For the sake of necessity, we assume that (C,A) is unobservable, and there is a matrix  $\widetilde{P}$  that makes the LMI (19) accurate. Since  $\widetilde{A}$  is not Hurwitz, we imply that all eigenvalues of  $-Q=\widetilde{A}^{\top}\widetilde{P}+\widetilde{P}\widetilde{A}$  are not negative, which leads to a

<sup>2&</sup>quot;o" represents the Hadamard product

contradiction since LMI (19) has no solution. This completes the proof.

**Remark 5:** It should be noticed that  $W^{L+2}$  in the shortcut connection of the NN plays an essential role in the construction of the above solution P by pole assignments. Moreover, from (i) and (ii), the solution P also be utilized to guarantee the existence of a reliable NN mapping  $\pi_{\theta}$ . Note that (C, A) is observable if A is Hurwitz. Then, we can take A = A by setting  $W^{L+2} = O$  from the NN mapping  $\pi_{\theta}$ , which means that the residual neural network defined in (2) will degenerate to a fully-connected NN. Therefore, Corollary 1 shows that the LMI (19) solution exists in this case.

**Corollary 1:** Let the assumptions (i) and (ii) are still satisfied. We set  $\alpha_{\sigma} = \mathbf{0}_{n_{\sigma}}$  but A = A, and corresponding matrices Q, P defined in Proposition 1. Then P is a solutions for LMI (19) if and only if A is Hurwitz.

*Proof:* The proof is a direct extension of Proposition 1.

The next theorem gives the necessary conditions to achieve the control target in Problem 1.2 by using the measurement  $\widehat{x}(t)$ . From (4)-(5), by utilizing the NN controller of the form  $u(t) = \pi_{\theta_2}(\hat{x})$ , it is not difficult to obtain

$$\begin{cases} \dot{x} = Ax + B\pi_{\theta_1}(\widehat{x}) \\ \dot{\widehat{x}} = A\widehat{x} + B\pi_{\theta_1}(\widehat{x}) + \pi_{\theta_2}\left(C(\widehat{x} - x)\right) \end{cases}$$
(20)

By denoting  $x_1 \triangleq x$ ,  $x_2 \triangleq \hat{x} - x$ , and  $\mathbf{x}^{\top} = [x_1^{\top}, x_2^{\top}]$ , equation (20) turns into

$$\frac{d\boldsymbol{x}}{dt} = \widehat{A}\boldsymbol{x} + v(\boldsymbol{x}),$$

where  $\widehat{A}=\operatorname{diag}\left(A,A\right)$  and  $v(\boldsymbol{x})=\begin{bmatrix}B\pi_{\theta_1}([I,I]\boldsymbol{x})\\\pi_{\theta_2}([O,C]\boldsymbol{x})\end{bmatrix}$ . Correspondingly, as K=2, we also treat  $\boldsymbol{x}(t)$  as an input variable of the NN mapping vector  $\boldsymbol{\pi}_{\boldsymbol{\theta}} = [\pi_{\theta_1}^{\perp}, \pi_{\theta_2}^{\perp}]^{\perp}$ 

**Theorem 2:** Consider two NN mappings  $\pi_{\theta_1}$  and  $\pi_{\theta_2}$  with parameters  $\theta_i = \left(L_i, n_{\sigma_i}, W_i^1, \cdots, W_i^{L_i+2}\right), i = 1, 2$ . Let parameter K in Lemma 2 be equal to 2, and  $T_1^1$ ,  $T_1^2$ ,  $T_2^1$ ,  $T_2^2$  in (17) are equal to [I, I], B, [O, C], I, respectively. We suppose that there exists a matrix  $\widehat{P} \in \mathcal{L}(\mathbf{R}^{2n_s})$  and  $\widehat{P} \succ O$ such that

$$\widehat{R_{\pi}}^{\top} \begin{bmatrix} \widehat{A}^{\top} \widehat{P} + \widehat{P} \widehat{A} & \widehat{P} \\ \widehat{P} & O \end{bmatrix} \widehat{R_{\pi}} + \widehat{R_{\xi}}^{\top} \mathbf{\Psi}(2)^{\top} \mathbf{M}(2) \mathbf{\Psi}(2) \widehat{R_{\xi}} \prec O,$$
(21)

where  $\widehat{R}_{\pi}$ ,  $\widehat{R}_{\xi}$ , and  $\Psi(2)$ , M(2) are defined in (17), and (18) as K=2, respectively. Then, the LTI system (4) is neural exponential observable and globally exponentially stable.

*Proof:* Consider the radially unbounded function V:  $\mathbf{R}^{2n_s} \to \mathbf{R}, \ \boldsymbol{x}(t) \mapsto \boldsymbol{x}^{\top}(t) P \boldsymbol{x}(t)$  as a candidate Lyapunov function for above system. Therefore, the time derivative of V along the trajectories of (20) is given by

$$\left. \frac{dV}{dt} \right|_{\boldsymbol{x}(t)} = [\star]^\top \left[ \begin{array}{cc} \widehat{A}^\top \widehat{P} + \widehat{P} \widehat{A} & \widehat{P} \\ \widehat{P} & O \end{array} \right] \left[ \begin{array}{cc} \boldsymbol{x}(t) \\ v(\boldsymbol{x}) \end{array} \right].$$

Due to the strictness of LMI (21) and Lemma 2, by left/right multipling the vector  $\left| \boldsymbol{x}^{\top}, \left( w_{\sigma}^{2} \right)^{\top} \right|$  and its transpose, we know that there exists  $\epsilon > 0$  such that for all  $x \in \mathbf{R}^{2n_s}$ ,

$$\begin{split} \frac{dV}{dt}\Big|_{\boldsymbol{x}(t)} &\leq -\underbrace{[\star]^{\top}\boldsymbol{\Psi}(2)^{\top}\mathbf{M}(2)\boldsymbol{\Psi}(2)\left[\begin{array}{c} \xi_{\sigma}^{2}(t) \\ w_{\sigma}^{2}(t) \end{array}\right]}_{\geq 0} -\epsilon\|\boldsymbol{x}(t)\|_{2}^{2}, \\ &\leq -\epsilon\|\boldsymbol{x}(t)\|_{2}^{2}. \end{split}$$

Similarly, we have

$$\left\|\boldsymbol{x}(t)\right\|_2 \leq \sqrt{\frac{\lambda_{\max}(\widehat{P})}{\lambda_{\min}(\widehat{P})}} e^{-\frac{\epsilon t}{2\lambda_{\max}(\widehat{P})}} \left\|\boldsymbol{x}(0)\right\|_2.$$

Notice that  $\mathbf{x}^{\top}(t) = [x_1(t)^{\top}, x_2(t)^{\top}]$  and that  $x_1(t) = x(t)$ , and  $x_2(t) = \hat{x}(t) - x(t)$ . It is easy to obtain that

$$||x(t)||_2 + ||x(t) - \widehat{x}(t)||_2 \le Me^{-\kappa t} \{||x(0)||_2 + ||\widehat{x}(0)||_2\},$$

where  $M=2\sqrt{\frac{2\lambda_{\max}(\widehat{P})}{\lambda_{\min}(\widehat{P})}}$ , and  $\kappa=\frac{\epsilon}{2\lambda_{\max}(\widehat{P})}$ . Hence, the system (4) is neural exponential observable, and the state x(t)converges to 0 as  $t \to \infty$  exponentially, which leads to the completeness of the proof.

Reasonably, the existence of solutions to LMI (21) needs to be taken into account, and below, we propose one class of solutions satisfying LMI (21).

**Proposition 2:** By setting  $\alpha_{\sigma_i} = \mathbf{0}_{n_{\sigma_i}}$ ,

- $\widetilde{A}_1=A+BW_1^{L_1+2},\ P_1=\int_0^\infty e^{\widetilde{A}_1^\top t}Q_1e^{\widetilde{A}_1t}dt$  with a diagonal matrix  $Q_1\succ O,$  and  $\widetilde{A}_2=A+W_2^{L_2+2}C,\ P_2=\int_0^\infty e^{\widetilde{A}_2^\top t}Q_2e^{\widetilde{A}_2t}dt$  with
- a diagonal matrix  $Q_2 \succ O$ ,

we assume that there exists  $\lambda_{\sigma}^2 > \mathbf{0}_{n^2}$  such that

- (iii)  $||M_1||_{\infty} + ||M_3||_{\infty} \leq \min_i(\widehat{q}_i)$ , where  $M_1 = -\widehat{P}\widehat{N_{\pi w}}$  $\begin{array}{l} \widehat{N_{\xi x}} \quad \text{$||M_3|| $\otimes \subseteq \lim_{t \to 0} (q_t)$, where $|M_1$ is the $i_{th}$ diagonal entry in $\widehat{Q} = \operatorname{diag}(P_1, P_2)$, and $M_3 = \left[ \begin{array}{cc} O & P_1 B W_1^{L_1 + 2} \\ \star & O \end{array} \right]$,} \end{array}$
- (iv)  $||M_1^\top||_{\infty} + ||M_2||_{\infty} \le 2 \min_i(\lambda_{\sigma,i})$ , where  $\lambda_{\sigma,i}$  is the  $i_{th}$ element of  $\lambda_{\sigma}^2$ ,  $M_2 = R_1 \widehat{N_{\varepsilon w}} + \widehat{N_{\varepsilon w}}^{\top} R_1$ .

Then LMI (21) has a solution  $\widehat{P}$  if and only if (C, A) is observable and (A, B) is controllable.

*Proof:* Sufficiency: Since (C, A) is observable, and (A,B) is controllable,  $\widetilde{A}_1=A+BW_1^{L_1+2}$  and  $\widetilde{A}_2=A+W_2^{L_2+2}C$  are two Hurwitz matrices by making  $W_1^{L_1+2}$  and  $W_2^{L_2+2}$  are pole assignment matrices. Subsequently, it is not difficult to verify that  $P_i$  and  $Q_i$  satisfy the Lyapunov equation  $-(A_i^{\top}P_i + P_iA_i) = Q_i, i = 1, 2$ . The matrices on the left side of LMI (21) can be expanded to

$$\widehat{R_{\pmb{\pi}}}^\top \left[ \begin{array}{cc} \widehat{A}^\top \widehat{P} + \widehat{P} \widehat{A} & \widehat{P} \\ \widehat{P} & O \end{array} \right] \widehat{R_{\pmb{\pi}}} = \left[ \begin{array}{cc} -\widehat{Q} + M_3 & \widehat{P} \widehat{N_{\pi w}} \\ \star & O \end{array} \right]$$

$$\widehat{R_{\xi}}^{\top} \mathbf{\Psi}(2)^{\top} \mathbf{M}(2) \mathbf{\Psi}(2) \widehat{R_{\xi}} = \begin{bmatrix} O & \widehat{N_{\xi x}}^{\top} R_1 \\ \star & \widehat{N_{\xi w}}^{\top} R_1 + R_1 \widehat{N_{\xi w}} \\ -2 \operatorname{diag}(\lambda_{\sigma}^2) \end{bmatrix}.$$

Hence, based on the assumptions (iii) and ((iv), the LMI (21) is satisfied due to the property of strict diagonal dominance.

Necessity: The proof is the same as step 2 in Proposition 1.

In the following sections, to make the content as concise as possible, we would not prove the existence of LMI solutions in detail once the conditions of observability or stabilization are satisfied since the proofs are similar to Proposition 1-2.

# B. Uncertainty is Effectively Dealt by Neural Observers

We construct an extended state,

$$x_{n+1}(t) = \mathcal{F}(t, \boldsymbol{x}, w),$$

for (8) and then redefine system (8) as follows

$$\begin{cases} \dot{\widetilde{x}} = \widetilde{\mathcal{A}}\widetilde{x} + \widetilde{L}(t, x, w, u), \\ y = \widetilde{c}\widetilde{x}, \end{cases}$$
 (22)

where  $\widetilde{\boldsymbol{x}} = [\boldsymbol{x}^\top, x_{n+1}]^\top$ ,  $\widetilde{\mathcal{A}} = (a_{ij})_{(n+1)\times(n+1)}$  is defined by

$$a_{ij} = \begin{cases} 1, & i+1=j \\ 0, & else \end{cases}, \ \widetilde{c} = [1, 0, \cdots, 0] \in \mathcal{L}(\mathbf{R}^{n+1}, \mathbf{R}),$$

$$\widetilde{L}(t, \boldsymbol{x}, w, u) = [0, \cdots, bu(t), \frac{d}{dt} \mathcal{F}(t, \boldsymbol{x}, w)]^{\top}.$$

Correspondingly, the output of neural observer (9) is redefined as  $\widehat{y} = \widetilde{c}[\widehat{x}^{\top}, \widehat{x}_{n+1}]^{\top}$ . Suppose that  $\mathcal{F}$  satisfies Assumption 2. Denote  $h(t) \triangleq \frac{d}{dt}\mathcal{F}(t, \boldsymbol{x}, w)$  and  $\eta_i \triangleq \epsilon^{-n-1+i}(x_i - \widehat{x}_i), i = 1, \cdots, n+1$ . Then, from (22) and (9) we derive an error system for (7) and (9):

$$\begin{cases} \epsilon \dot{\eta}_i = \eta_{i+1} - \pi_{\theta_i}(\widetilde{c}\boldsymbol{\eta}), & i = 1, 2, \cdots, n, \\ \epsilon \dot{\eta}_{n+1} = -\pi_{\theta_{n+1}}(\widetilde{c}\boldsymbol{\eta}) + \epsilon h(t), \end{cases}$$
 (23)

where  $\eta = [\eta_1, \cdots, \eta_{n+1}]^{\top}$ . From the above error system (23), as K = n+1 in Lemma 2, we treat  $\eta$  as the input of NN mapping vector  $\boldsymbol{\pi}_{\boldsymbol{\theta}} = [\pi_{\theta_1}, \cdots, \pi_{\theta_{n+1}}]^{\top}$  by setting  $T_1^i = \widetilde{c}, T_2^i = 1, \ i = 1, \cdots, n+1$ . Now, we formally propose the result for Problem 2.1.

**Theorem 3:** Consider n+1 NN mappings  $\pi_{\theta_i}$  with parameters  $\theta_i = \left(L_i, n_{\sigma_i}, W_i^1, \cdots, W_i^{L_i+2}\right), \ i=1,\cdots,n+1$ . We assume that

- (1) K = n + 1 in Lemma 2, and  $T_i^1 = \tilde{c}, T_i^2 = 1, i = 1, \dots, n + 1$  in (17),
- (2) there exists a matrix  $P \in \mathcal{L}(\mathbf{R}^{n+1})$  and  $P \succ O$  such that

$$\widehat{R_{\pi}}^{\top} \begin{bmatrix} \widetilde{\mathcal{A}}^{\top} P + P \widetilde{\mathcal{A}} & -P \\ -P & O \end{bmatrix} \widehat{R_{\pi}} + \widehat{R_{\varepsilon}}^{\top} \Psi(n+1)^{\top} \mathbf{M}(n+1) \Psi(n+1) \widehat{R_{\varepsilon}} \prec O.$$
(24)

Then we have the following results:

- (I) Neural observability: for all  $x(0) \in \mathbb{R}^n$ ,  $\|x(t) \widehat{x}(t)\|_2 \to 0$  as  $\mu \to 0^+$  for  $t \in \mathcal{T}_{>T}$  with T > 0.
- (II) Total uncertainty  $x_{n+1} = F(t, \boldsymbol{x}, w)$  can be measured by  $\widehat{x}_{n+1}$  as  $\epsilon \to 0^+$ , i.e.,  $\lim_{\epsilon \to 0^+} |x_{n+1} \widehat{x}_{n+1}| = 0$ .

*Proof*: Firstly, by constructing that  $V_0: \mathbf{R}^{n+1} \to \mathbf{R}, \boldsymbol{\eta}(t) \mapsto \boldsymbol{\eta}(t)^\top P \boldsymbol{\eta}(t)$ , we denote  $\lambda_1 = \lambda_{\min}(P)$  and  $\lambda_2 = \lambda_{\max}(P)$  and compute the time derivative of  $V_0(\boldsymbol{\eta})$  along (23) as

$$\begin{split} \frac{dV_0}{dt}\Big|_{\boldsymbol{\eta}(t)} = & \epsilon^{-1} [\star]^\top \left[ \begin{array}{cc} \widetilde{\mathcal{A}}^\top P + P \widetilde{\mathcal{A}} & -P \\ -P & O \end{array} \right] \left[ \begin{array}{c} \boldsymbol{\eta}(t) \\ \boldsymbol{\pi}_{\boldsymbol{\theta}}(\boldsymbol{\eta}) \end{array} \right] \\ & + \frac{\partial V_0}{\partial n_{n+1}} h(t), \end{split}$$

Due to the assumption of LMI (24) and Lemma 2, we imply that there exists  $\lambda_3 > 0$  such that

$$[\star]^{\top} \begin{bmatrix} \widetilde{\mathcal{A}}^{\top} P + P \widetilde{\mathcal{A}} & -P \\ -P & O \end{bmatrix} \begin{bmatrix} \boldsymbol{\eta}(t) \\ \boldsymbol{\pi}_{\boldsymbol{\theta}}(\boldsymbol{\eta}) \end{bmatrix} \leq -\lambda_{3} \| \boldsymbol{\eta}(t) \|_{2}^{2}$$

$$- \underbrace{[\star]^{\top} \boldsymbol{\Psi}(n+1)^{\top} \mathbf{M}(n+1) \boldsymbol{\Psi}(n+1) \begin{bmatrix} \xi_{\sigma}^{n+1}(t) \\ w_{\sigma}^{n+1}(t) \end{bmatrix}}_{\geq 0}.$$

Moreover, we obtain that

$$\frac{dV_0}{dt}\Big|_{\boldsymbol{\eta}(t)} \le -\epsilon^{-1}\lambda_3 \|\boldsymbol{\eta}(t)\|_2^2 + \frac{\partial V_0}{\partial \eta_{n+1}} h(t), 
\le -\epsilon^{-1} \frac{\lambda_3}{\lambda_2} V_0(\boldsymbol{\eta}) + \frac{\partial V_0}{\partial \eta_{n+1}} h(t),$$
(25)

where

$$h(t) = \mathcal{F}_t + \sum_{i=1}^{n-1} x_{i+1} \mathcal{F}_{x_i} + bu \mathcal{F}_{x_n} + \dot{w} \mathcal{F}_w.$$

Secondly, by retrieving Assumption 2 about the boundedness of x and u(t) and continuity of  $\chi(x,w)$ , we use the the HeineBorel theorem to get that the uncertain term h(t) is also bounded, i.e.,  $|h(t)| \leq M_0$  Hence, by combining the last term with  $dV_0/dt$ , we get that

$$\frac{dV_0}{dt}\Big|_{\boldsymbol{\eta}(t)} \le -\frac{\lambda_3}{\epsilon \lambda_2} V_0(\boldsymbol{\eta}) + 2\lambda_2 M_0 \|\boldsymbol{\eta}\|_2, 
\le -\frac{\lambda_3}{\epsilon \lambda_2} V_0(\boldsymbol{\eta}) + \frac{2\lambda_2}{\sqrt{\lambda_1}} M_0 \sqrt{V_0(\boldsymbol{\eta})},$$

 $\Rightarrow$ 

$$\frac{d\sqrt{V_0}}{dt}\Big|_{\boldsymbol{n}(t)} \leq -\epsilon^{-1} \frac{\lambda_3}{2\lambda_2} \sqrt{V_0(\boldsymbol{\eta})} + \frac{\lambda_2}{\sqrt{\lambda_1}} M_0.$$

Applying the Gronwall-Bellman inequality again implies that

$$\sqrt{V_0(\boldsymbol{\eta})} \le \left(\sqrt{V_0(\boldsymbol{\eta}(0))} - M_1\right) e^{-\frac{\lambda_3}{2\epsilon\lambda_2}t} + M_1, \qquad (26)$$

where  $M_1 = \epsilon \frac{2\lambda_2^2}{\lambda_3\sqrt{\lambda_1}} M_0$ . To be specific, if  $\epsilon \to 0^+$ , we get

$$\sqrt{V_0(\boldsymbol{\eta}(0))}e^{-\frac{\lambda_3}{2\epsilon\lambda_2}t} = \left(\sum_{i=1}^n \left| \frac{(x_i(0) - \widehat{x}_i(0))}{\epsilon^{n+1-i}} \right|^2 \right)^{\frac{1}{2}} e^{-\frac{\lambda_3}{2\epsilon\lambda_2}t}$$

$$\to 0^+$$

Therefore, as  $\epsilon \to 0^+$ , we obtain that for  $t \in \mathcal{T}_{>T}$ ,

$$\|\boldsymbol{x} - \widehat{\boldsymbol{x}}\|_2 = \left(\sum_{i=1}^n |\epsilon^{n+1-i}\eta_i|^2\right)^{\frac{1}{2}} \le \epsilon \|\boldsymbol{\eta}\|_2 \to 0^+.$$

Moreover,  $|x_{n+1} - \widehat{x}_{n+1}| = |\eta_{n+1}| \le ||\eta||_2 \to 0^+$ . These complete the whole proof.

**Remark 6:** For (24), due to the observability of  $(\widetilde{c}, \widetilde{\mathcal{A}})$ , we can select  $W^{L+2} = [W_1^{L_1+2}, \cdots, W_{n+1}^{L_{n+1}+2}]^{\top}$  as a pole assignment matrix such that  $\mathcal{A} + \widehat{R_{\pi x}} = \mathcal{A} + W^{L+2}\widetilde{c}$  is Hurwitz, where  $\widehat{R_{\pi x}}$  is a block matrix of  $\widehat{R_{\pi}}$ . Then, by a similar analysis with Proposition 1-2, it is not difficult to check that LMI (24) has solutions under some given conditions.

To decrease the computational complexity for LMI (24) and avoid the consequences of sparsity [30], [31], we can take that

the NN mappings in (9) are identical, i.e.,  $\pi_{\theta_i}(\cdot) = \pi_{\theta}(\cdot), i = 1, \dots, n+1$ . Moreover, the gains of the NN mapping are equal to  $\epsilon^{n+1-i}b_i$ , i.e.,

$$\begin{cases} \dot{\widehat{x}}_i = \widehat{x}_{i+1} + \epsilon^{n-i} b_i \pi_{\theta} (\epsilon^{-n} (y - \widehat{y})), & i = 1, \dots, n, \\ \dot{\widehat{x}}_{n+1} = \epsilon^{-1} b_{n+1} \pi_{\theta} (\epsilon^{-n} (y - \widehat{y})) + bu, \\ \widehat{y} = c \widehat{x}. \end{cases}$$

Then we present the following corollary to solve the sparsity of LMI (24).

**Corollary 2:** We consider this NN map  $\pi_{\theta}$  with one parameter  $\theta = (L, n_{\sigma}, W^1, \dots, W^{L+2})$  and re-assume

- (1) K = 1 in Lemma 2, and  $T_1^1 = \tilde{c}, T_1^2 = 1$  in (17),
- (2) Let b be the vector  $[b_1, \cdots, b_{n+1}]^{\top}$ . Suppose that there exists a matrix  $P \in \mathcal{L}(\mathbf{R}^{n+1})$  and  $P \succ O$  such that

$$\widehat{R}_{\pi}^{\top} \begin{bmatrix} \widetilde{\mathcal{A}}^{\top} P + P \widetilde{\mathcal{A}} & -Pb \\ -Pb & O \end{bmatrix} \widehat{R}_{\pi} + \widehat{R}_{\xi}^{\top} \mathbf{\Psi}(1)^{\top} \mathbf{M}(1) \mathbf{\Psi}(1) \widehat{R}_{\xi} \prec O,$$
(27)

where  $\widehat{R}_{\pi}$ ,  $\widehat{R}_{\xi}$ ,  $\Psi(1)$  and  $\mathbf{M}(1)$  are defined in (17) and (18).

Then we can still get three results in Theorem 3, including neural observability, and the measurement of the total uncertainty  $\mathcal{F}(t, \boldsymbol{x}, w)$ .

*Proof:* By directly extending the proof of Theorem 3, the proof of Corollary 2 can be obtained trivially. ■

# C. Mismatched Uncertainties in Linear Systems Can be Dealt by Neural Observers

Before showing Theorem 4 for Problem 3.1, we introduce a necessary lemma. Furthermore, finally, we present the last Theorem for systems (10).

**Lemma 3:** Let  $D_0$  and  $D_1$  be two symmetric matrices in which  $D_1 \succ O$ . Then  $D_1$  with a small perturbation  $\epsilon D_0$  is still positive definite as long as  $\epsilon \in \left(0, \frac{\lambda_{\min}(D_1)}{\|D_0\|_2}\right)$ , i.e.,  $D_1 + \epsilon D_0 \succ O$ .

*Proof:* The proof is given in Appendix I.

**Theorem 4:** Consider two NN mappings  $\pi_{\theta_1}$  and  $\pi_{\theta_2}$  with parameter  $\theta_i = \left(L_i, n_{\sigma_i}, W_i^1, \cdots, W_i^{L_i+2}\right), \ i = 1, 2.$  Let parameter K in Lemma 2 be equal to 2, and  $T_i^1, T_i^2$  in (17) are equal to  $\mathbf{C}$ , I, respectively. We suppose that there exists a positive definite matrix  $\mathbf{P} \in \mathcal{L}(\mathbf{R}^{2n_s})$  such that

$$D_{1} \triangleq -\widehat{R_{\pi}}^{\top} \begin{bmatrix} \mathbf{I}^{\top} \mathbf{P} + \mathbf{P} \mathbf{I} & -\mathbf{P} \\ -\mathbf{P} & O \end{bmatrix} \widehat{R_{\pi}} - \widehat{R_{\xi}}^{\top} \mathbf{\Psi}(2)^{\top} \mathbf{M}(2) \mathbf{\Psi}(2) \widehat{R_{\xi}} \succ O$$
(28)

and define

$$D_0 \triangleq -\widehat{R_{\pi}}^{\top} \begin{bmatrix} \mathbf{A}^{\top} \mathbf{P} + \mathbf{P} \mathbf{A} & -\mathbf{P} \\ -\mathbf{P} & O \end{bmatrix} \widehat{R_{\pi}}$$

with  $\mathbf{A} \triangleq \begin{bmatrix} A & O \\ O & O \end{bmatrix}$  and  $\mathbf{I}$  is defined in Assumption 3. Under

Assumption 3 aforementioned, then for all  $\epsilon \in \left(0, \frac{\lambda_{\min}(D_1)}{\|D_0\|_2}\right)$ , the system (10) is neural observable in the following sense:

- $\underline{\lim}_{\epsilon \to 0^+} \|x_i(t) \hat{x}_i(t)\|_2 = 0$  for all  $t \in \mathcal{T}_{>a}, \ a > 0$ .
- $\overline{\lim}_{t\to\infty} ||x_i(t) \hat{x}_i(t)||_2 \le O(\epsilon^{2-i})$

*Proof:* Firstly, we denote  $x_1(t) = x(t)$ ,  $x_2(t) = \mathcal{K}(t)$ , then the system (10) can be rewritten into

$$\begin{cases} \dot{x}_1 = Ax_1 + Bu + x_2, \\ \dot{x}_2 = \nabla_t \mathcal{K}, \\ y = \mathbf{C} \begin{bmatrix} x_1 \\ x_2 \end{bmatrix} \end{cases}$$

By denoting the errors  $e_i(t)=x_i(t)-\widehat{x}_i(t)$  and  $\eta_i(t)=\frac{e_i(\epsilon t)}{\epsilon^2-i}$ , we have the following formulation:

$$\begin{bmatrix} \dot{\eta}_1 \\ \dot{\eta}_2 \end{bmatrix} = \underbrace{\begin{bmatrix} \epsilon A & I \\ O & O \end{bmatrix}}_{\mathbf{B} = \epsilon \mathbf{A} + \mathbf{I}} \underbrace{\begin{bmatrix} \eta_1 \\ \eta_2 \end{bmatrix}}_{\boldsymbol{\eta}(t)} - \underbrace{\begin{bmatrix} \pi_{\theta_1}(\mathbf{C}\boldsymbol{\eta}) \\ \pi_{\theta_2}(\mathbf{C}\boldsymbol{\eta}) \end{bmatrix}}_{\boldsymbol{\pi}_{\boldsymbol{\theta}}(t)} + \begin{bmatrix} 0 \\ \epsilon \nabla_t \mathcal{K} \end{bmatrix}.$$

In form,  $\eta(t)$  can be considered as the input of NN mapping vector  $\boldsymbol{\pi}_{\boldsymbol{\theta}}$ . From Assumption 3, it is easy to check that  $\|\nabla_t \mathcal{K}(t)\|_2 \leq M$  with M>0. Assume that the Lyapunov function  $V(\boldsymbol{\eta}) = \boldsymbol{\eta}^{\top} \mathbf{P} \boldsymbol{\eta}$  and  $\epsilon \in \left(0, \frac{\lambda_{\min}(D_1)}{\|D_0\|_2}\right)$ . Then, by applying Lemma 2-3 and  $D_1 \succ O$ , we denote  $\lambda_1 = \lambda_{\min}(P)$  and  $\lambda_2 = \lambda_{\max}(P)$  and consequently have the following inequality:

$$\frac{dV}{dt}\Big|_{\boldsymbol{\eta}(t)} \leq [\star]^{\top} \begin{bmatrix} \mathbf{B}^{\top} \mathbf{P} + \mathbf{P} \mathbf{B} & -\mathbf{P} \\ -\mathbf{P} & O \end{bmatrix} \begin{bmatrix} \boldsymbol{\eta}(t) \\ \boldsymbol{\pi}_{\boldsymbol{\theta}}(t) \end{bmatrix} + \frac{\partial V}{\partial \eta_{2}} \epsilon \nabla_{t} \mathcal{K}(t)$$

$$\leq - [\star]^{\top} \boldsymbol{\Psi}(2)^{\top} \mathbf{M}(2) \boldsymbol{\Psi}(2) \begin{bmatrix} \xi_{\sigma}^{2}(t) \\ w_{\sigma}^{2}(t) \end{bmatrix}$$

$$- \kappa \|\boldsymbol{\eta}(t)\|_{2}^{2} + 2\epsilon M \lambda_{2} \|\boldsymbol{\eta}(t)\|_{2}$$

$$\leq - \frac{\kappa}{\lambda_{2}} V(\boldsymbol{\eta}) + \frac{2\epsilon M \lambda_{2}}{\sqrt{\lambda_{1}}} \sqrt{V(\boldsymbol{\eta})}.$$
(29)

Uniformly, by using Gronwall-Bellman inequality, we derive that

$$||e_{i}(t)||_{2} \leqslant \epsilon^{2-i} \left[ \sqrt{\frac{V(\boldsymbol{\eta}(0))}{\lambda_{1}}} e^{-\frac{\kappa t}{2\lambda_{2}\epsilon}} + \frac{2\epsilon M \lambda_{2}^{2}}{\lambda_{1}\kappa} (1 - e^{-\frac{\kappa t}{2\lambda_{2}\epsilon}}) \right],$$

$$\to 0 \qquad (as \ \epsilon \to 0^{+}).$$

This completes the proof.

#### VI. NUMERICAL EXPERIMENTS

In the following examples, the LMI (21),(24), and (28) are solved using the LMI Toolbox in MATLAB R2021a.

#### A. Linearized Aerodynamic Models of the X-29A Aircraft

In order to demonstrate the application effect of the proposed neural observer in linear systems, we implement the neural control framework combining the neural observer (5) and the NN controller (6) to the X-29A aircraft, which is formulated in the following state-space form:

$$\begin{cases} \dot{x} = Ax + Bu, \\ y = Cx, \end{cases}$$

where the nominal system matrices A,B, and C can be obtained from Table 9 in [32] and  $x(t) \in \mathbf{R}^4$ . The NNs  $\pi_{\theta_i}, i=1,2$  in (5) and (6) are parameterized by three hidden layers with  $n_1=n_2=n_3=3$  and ReLU as the activation function for both layers. System response and the output of

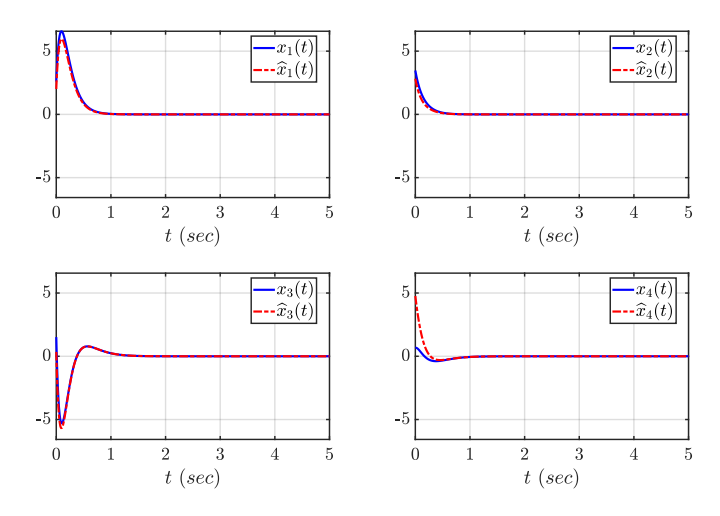


Fig. 6. The state trajectories of X-29 aircraft under the neural control framework.

the neural observer are depicted in Fig. 6. It can be shown that the states  $x_i(t), i=1,\cdots,4$  both converge to 0, and the states  $x_i(t), i=1,\cdots,4$  are well estimated by  $\widehat{x}_i(t), i=1,\cdots,4$ , respectively.

# B. A Second-order Nonlinear Model of the Inverted Pendulum

Next, to show the effectiveness of neural observers for high-order nonlinear systems, we consider the control of the nonlinear inverted pendulum system formulated by  $\ddot{\theta}(t) = \frac{mgl\sin(\theta(t)) - \varsigma_0\dot{\theta}(t) + u(t) + w(t)}{ml^2}$ , where  $\theta(t)$  is the angular position (rad), and  $m, l, \varsigma_0$  represent the mass (kg), the length (m), and the friction coefficient (Nms/rad), respectively, and  $w(t) = \sum_{i=1}^p a_i \sin b_i t$  is the external disturbance. By denoting  $x_1 = \theta$  and  $x_2 = \dot{\theta}$ , we rewrite state-space form for inverted pendulum system

$$\begin{cases} \dot{x_1} = x_2, \\ \dot{x_2} = \frac{mgl\sin(x_1) - \varsigma_0 x_2 + u(t) + w(t)}{ml^2}, \\ y = x_1, \end{cases}$$

The following neural observer is designed:

$$\begin{cases} \dot{\widehat{x}}_i = \widehat{x}_{i+1} + \epsilon^{2-i} \pi_{\theta_i} (\epsilon^{-2} (y - \widehat{y})), & i = 1, 2, \\ \dot{\widehat{x}}_3 = \epsilon^{-1} \pi_{\theta_3} (\epsilon^{-2} (y - \widehat{y})) + bu, \\ \widehat{y} = \widehat{x}_1, \end{cases}$$

and the neural observer-based feedback control input u(t) (Nm) is designed by  $u(t) = \rho \sum_{i=1}^{2} k_i \operatorname{sat}_{M_i}(\rho^{n-i} \widehat{x}_i(t)) - \operatorname{sat}_{M_3}(\widehat{x}_3(t))$ .

Without loss of generality, we set m=1, l=1, and  $\varsigma_0=0.5$ . In the corresponding neural observer (9), we design that (i) the gain  $\epsilon=0.01$ ; (ii) the NN  $\pi_{\theta_i}$ ,  $i=1,\cdots,3$  are

parameterized by two hidden layers with  $n_1=3$  and  $n_2=2$  and tanh as the activation function for both layers. As for the neural control law, we design that  $\rho=1$ ,  $k_1=-25, k_2=-10$ , and  $M_1=M_2=M_3=10$  (More details about the design of parameters can be seen in [24]). From Fig. 7-8, we can conclude that the neural observer is effective for tracking not only the states  $x_1, x_2$  but also the extended state  $x_3$  (total disturbance).

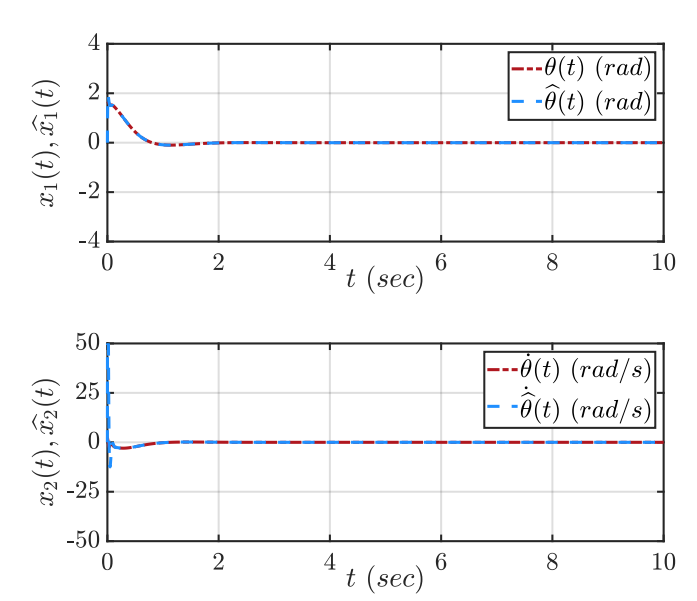


Fig. 7. The state trajectories of the inverted pendulum under the neural observer.

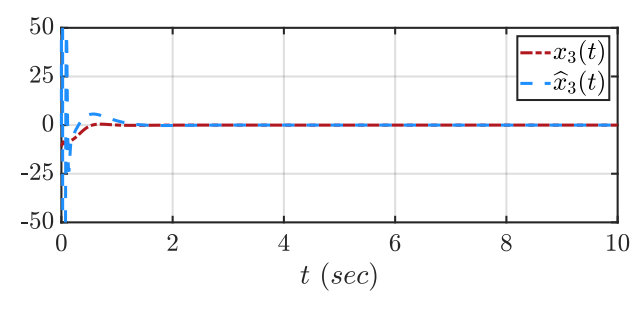


Fig. 8. The trajectory of extended state  $x_3 = \frac{mgl\sin(x_1) - \varsigma_0 x_2 + w(t)}{ml^2}$  of the inverted pendulum under the neural observer.

# C. The Dynamics of the Four-wheel Steering Vehicle

Finally, we implement the proposed neural observers (11) to the four-wheel steering vehicle, which is modeled as a linear system with mismatched uncertainties as follows [33]:

$$\begin{cases} \dot{x} = Ax + Bu + \mathcal{K}(x, w, t), \\ y = Cx, \end{cases}$$

where  $x=[e,\dot{e},\Delta\psi,\dot{\Delta\psi}],~C=I,~A,B,\mathcal{K}(x,w,t)$  are defined by

$$A = \begin{bmatrix} 0 & 1 & 0 & 0 \\ 0 & \frac{C_{\alpha f} + C_{\alpha r}}{mU} & -\frac{C_{\alpha f} + C_{\alpha r}}{m} & \frac{aC_{\alpha f} - bC_{\alpha r}}{mU} \\ 0 & 0 & 0 & 1 \\ 0 & \frac{aC_{\alpha f} - bC_{\alpha r}}{I_z U} & -\frac{aC_{\alpha f} - bC_{\alpha r}}{I_z} & \frac{a^2C_{\alpha f} + b^2C_{\alpha r}}{I_z U} \end{bmatrix},$$

$$B = \begin{bmatrix} 0 & 0 \\ -\frac{C_{\alpha f}}{m} & -\frac{C_{\alpha r}}{m} \\ 0 & 0 \\ -\frac{aC_{\alpha f}}{I_z} & \frac{bC_{\alpha f}}{I_z} \end{bmatrix}, \mathcal{K}(\cdot) = \begin{bmatrix} 0 \\ \frac{aC_{\alpha f} - bC_{\alpha r} - mU^2}{m} \\ 0 \\ \frac{a^2C_{\alpha f} + b^2C_{\alpha r}}{I_z} \end{bmatrix} \frac{1}{\rho_c}.$$

The states  $(e, \Delta \psi)$  in x are defined as the perpendicular distance to the lane edge and the angle between the tangent to the straight section of the road. For simplicity, we denote that  $x = [x_1, \cdots, x_4]^{\top}$ . The parameters  $C_{\alpha f}, C_{\alpha r}, m, U, I_z, a, b$  represent the front cornering stiffness (N/rad), rear cornering stiffness (N/rad), mass (kg), longitudinal velocity (m/s), the moment of inertia  $(kg/m^2)$ , distances from vehicle center of gravity to the front axle and rear axle, respectively, which are chosen to the nominal values obtained from Appendix A in [33]. The constant road curvature  $\rho_c$  in  $\mathcal{K}(\cdot)$  can be chosen to be 400 (meters).

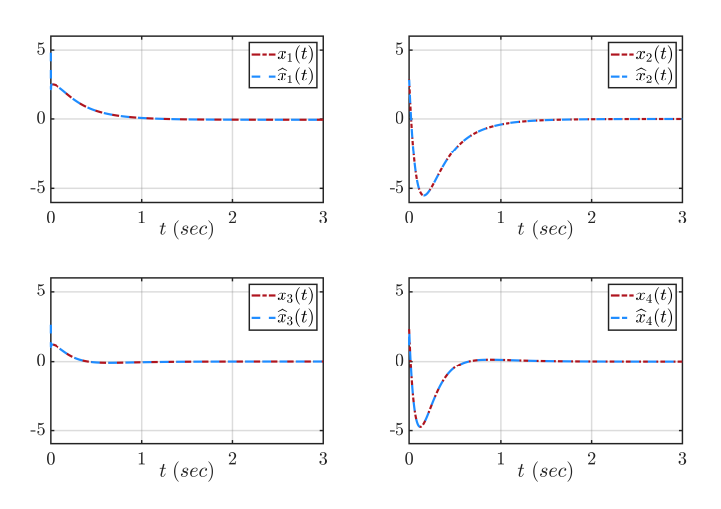


Fig. 9. The trajectory of each state  $x_i(t)$ ,  $i=1,\cdots,4$  of the fourwheel steering wehicle under the neural observer.

Again, the corresponding neural observer (11) is designed by (i) the NNs  $\pi_{\theta_i}, i=1,2$  are parameterized by by three hidden layers with  $n_1=n_2=n_3=3$  and Leaky ReLU as the activation function for both layers; (ii) the gain  $\epsilon$  is given by  $\epsilon \in \left(0, \frac{\lambda_{\min}(D_1)}{\|D_0\|_2}\right)$ . In our experiments, we calculate that  $\frac{\lambda_{\min}(D_1)}{\|D_0\|_2}=0.00529$ , and therefore we select that  $\epsilon=0.005$ . The control input is given by the output-feedback control u=Ky, where K is designed by the matrix A+BK is Hurwitz. Hence, it is easy to check that the state x and the input u are bounded.

In Fig. 9, we show that each state  $x_i, i=1,\cdots,4$  is well-estimated by  $\widehat{x}_i, i=1,\cdots,4$  from the neural observer. In Fig. 10, although the estimation states  $\widehat{x}_i, i=5,\cdots,8$  lead to a peaking phenomenon, each component of the extended

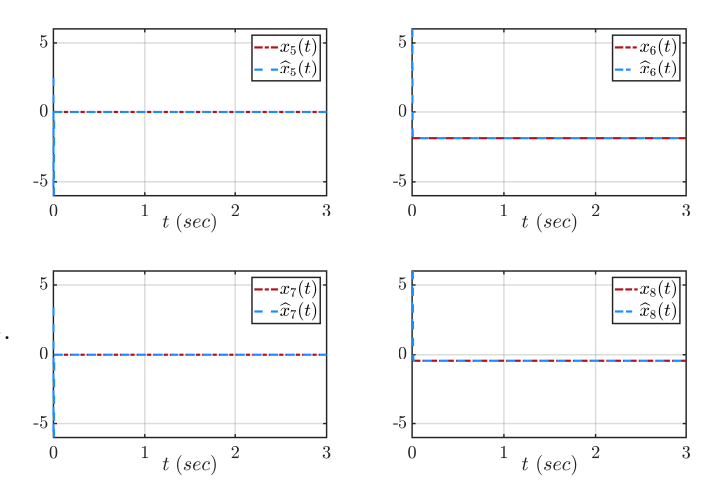


Fig. 10. The estimation of the extended state  $[x_5,\cdots,x_8]^{\top}=\mathcal{K}(x,w,t)$  of the four-wheel steering vehicle under the neural observer.

state  $x_i$ ,  $i = 5, \dots, 8$  could also be well-estimated by  $\widehat{x}_i$ ,  $i = 5, \dots, 8$  after a very short time, respectively.

#### VII. CONCLUSION

Machine learning meets control theory is always a topic worth discussing. In this paper, we make a new attempt: we introduce the residual neural network into the design of the observer, called the neural observer, and give the necessary proofs of convergence.

In this paper, we proposed a new framework to design the neural observer for systems, including linear systems and two classes of nonlinear systems with some mild assumptions. The strength of this neural observer relies on the representation of the capability of NNs. For linear systems, high-order nonlinear systems (which can be transformed into the form of integralchain systems), and linear systems with unmatched uncertainties, we provided a particular form of neural observers for each class of systems, respectively. In linear systems, by combing the recent NN controller proposed in [16], we showed that the observer could be used in global feedback stabilization. Finally, by using QCs to bound the nonlinear activation functions in NNs, we provided the corresponding LMI conditions for each system setting to achieve neural observability (according to Definition 1). On the other hand, it has also been shown that the observability of system matrices is a necessary condition for the existence of solutions of the aforementioned LMIs.

# A. Future Work and Discussion

Due to the generality of the introduced framework, it would be of interest to generalize the neural observer for the model class under consideration. On the one hand, for instance, one can consider larger classes of systems, such as polynomial systems. On the other hand, with some prior knowledge of the system, we can transform the system into special structures, such as the following Gauthier-Kupcas observability canonical form [34]:

$$\dot{x}_i = f_i\left(oldsymbol{x}_i, x_{i+1}, u\right)$$
 $\dot{x}_n = f_n\left(oldsymbol{x}_n, u\right) \quad , \quad ext{with } oldsymbol{x}_i = \left[x_1, \dots, x_i\right]^{\top}.$ 
 $y = h\left(x_1, u\right)$ 

Furthermore, we informally indicate that the global sector boundedness regarding activation functions introduced in Section IV is so "strict" that some information from activation functions may not be exploited fully. In detail, the following Fig. 11 shows the global sector using the tanh function as an example. Although we can describe the activation function

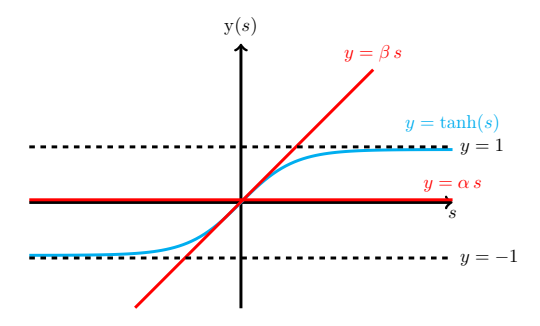


Fig. 11. Sector constraints on tanh(s)

 $y=\tanh(s)$  roughly by using the open region formed by two straight lines  $y=\alpha s, y=\beta s$  passing through the origin, some geometric information about the activation function, such as  $\lim_{s\to+\infty}\tanh(s)=1, \lim_{s\to-\infty}\tanh(s)=-1, \lim_{s\to\infty}\frac{d}{ds}\tanh(s)=0$ , is not fully reflected in Lemma 1-2 during this characterization process. Since the LMIs (19), (21), (24), and (28) are based on Lemma 1-2, the most direct consequence is that we would miss some NNs that do not satisfy the LMIs as mentioned earlier but can still be used in the design of neural observers.

Intuitively, we use the piecewise sectors shown in Fig. 12 to characterize the nonlinear activation function in the NN, which may make better use of geometric information to improve the results. The question, therefore, arises whether we can find constraint conditions from the piecewise sectors boundedness that can be utilized in neural observers.

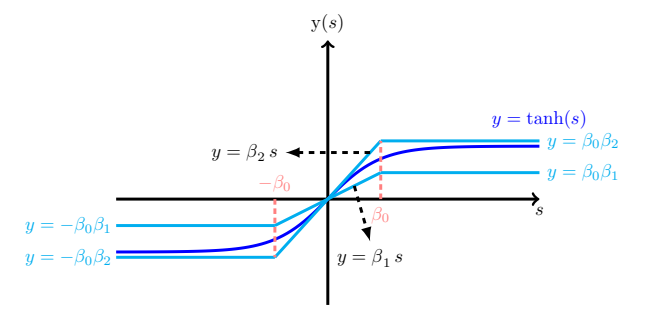


Fig. 12. Piecewise sector constraints on  $\tanh(s)$ : for  $s \in [-\beta_0, \beta_0]$ , we have  $(\tanh(s) - \beta_0 s) (\beta_1 s - \tanh(s)) \ge 0$ ; for  $|s| > \beta_0$ , we have  $(\tanh(s) - \mathrm{sign}(s)\beta_0\beta_2) (\mathrm{sign}(s)\beta_0\beta_1 - \tanh(s)) \ge 0$ .

#### REFERENCES

 P. J. Werbos, "Neural networks for control and system identification," in *Proceedings of the 28th IEEE Conference on Decision and Control*, pp. 260–265, 1989.

- [2] A. U. Levin and K. S. Narendra, "Control of nonlinear dynamical systems using neural networks: Controllability and stabilization," *IEEE Transactions on neural networks*, vol. 4, no. 2, pp. 192–206, 1993.
- [3] A. U. Levin and K. S. Narendra, "Control of nonlinear dynamical systems using neural networks. ii. Observability, identification, and control," *IEEE transactions on neural networks*, vol. 7, no. 1, pp. 30–42, 1996.
- [4] S. S. Ge, C. C. Hang, T. H. Lee, and T. Zhang, Stable adaptive neural network control, vol. 13. Springer Science & Business Media, 2013.
- [5] G. E. Karniadakis, I. G. Kevrekidis, L. Lu, P. Perdikaris, S. Wang, and L. Yang, "Physics-informed machine learning," *Nature Reviews Physics*, vol. 3, no. 6, pp. 422–440, 2021.
- [6] J. Z. Kolter and G. Manek, "Learning stable deep dynamics models," Advances in neural information processing systems, vol. 32, 2019.
- [7] L. Lu, P. Jin, G. Pang, Z. Zhang, and G. E. Karniadakis, "Learning nonlinear operators via deeponet based on the universal approximation theorem of operators," *Nature Machine Intelligence*, vol. 3, no. 3, pp. 218–229, 2021.
- [8] J. Han, A. Jentzen, and E. Weinan, "Solving high-dimensional partial differential equations using deep learning," *Proceedings of the National Academy of Sciences*, vol. 115, no. 34, pp. 8505–8510, 2018.
- [9] W. Hu, J. Long, Y. Zang, J. Han, et al., "Solving optimal control of rigidbody dynamics with collisions using the hybrid minimum principle," arXiv preprint arXiv:2205.08622, 2022.
- [10] L. Böttcher, N. Antulov-Fantulin, and T. Asikis, "AI Pontryagin or how artificial neural networks learn to control dynamical systems," *Nature Communications*, vol. 13, no. 1, pp. 1–9, 2022.
- [11] Q. Li, L. Chen, C. Tai, and W. E, "Maximum principle based algorithms for deep learning," *Journal of Machine Learning Research*, vol. 18, no. 165, pp. 1–29, 2018.
- [12] L. Lessard, B. Recht, and A. Packard, "Analysis and design of optimization algorithms via integral quadratic constraints," SIAM Journal on Optimization, vol. 26, no. 1, pp. 57–95, 2016.
- [13] T. Lin and M. I. Jordan, "A control-theoretic perspective on optimal high-order optimization," *Mathematical Programming*, pp. 1–47, 2021.
- [14] L. El Ghaoui, F. Gu, B. Travacca, A. Askari, and A. Tsai, "Implicit deep learning," SIAM Journal on Mathematics of Data Science, vol. 3, no. 3, pp. 930–958, 2021.
- [15] Z. Chen, Q. Li, and Z. Zhang, "Towards robust neural networks via close-loop control," in *International Conference on Learning Represen*tations, 2020.
- [16] H. Yin, P. Seiler, and M. Arcak, "Stability analysis using quadratic constraints for systems with neural network controllers," *IEEE Transactions on Automatic Control*, vol. 67, no. 4, pp. 1980–1987, 2022.
- [17] P. Pauli, J. Köhler, J. Berberich, A. Koch, and F. Allgöwer, "Offset-free setpoint tracking using neural network controllers," in *Proceedings of* the 3rd Conference on Learning for Dynamics and Control, vol. 144, pp. 992–1003, PMLR, 2021.
- [18] J. Han, "From pid to active disturbance rejection control," *IEEE Transactions on Industrial Electronics*, vol. 56, no. 3, pp. 900–906, 2009.
- [19] B.-Z. Guo and Z.-L. Zhao, Active disturbance rejection control for nonlinear systems: An introduction. John Wiley & Sons, 2016.
- [20] L. B. Freidovich and H. K. Khalil, "Performance recovery of feedback-linearization-based designs," *IEEE Transactions on Automatic Control*, vol. 53, no. 10, pp. 2324–2334, 2008.
- [21] K. Hornik, "Approximation capabilities of multilayer feedforward networks," *Neural Networks*, vol. 4, no. 2, pp. 251–257, 1991.
- [22] K. He, X. Zhang, S. Ren, and J. Sun, "Deep residual learning for image recognition," in 2016 IEEE Conference on Computer Vision and Pattern Recognition (CVPR), pp. 770–778, 2016.
- [23] C. E. Rasmussen and C. K. I. Williams, Gaussian Processes for Machine Learning. The MIT Press, 2005.
- [24] Z.-L. Zhao and B.-Z. Guo, "Active disturbance rejection control approach to stabilization of lower triangular systems with uncertainty," *International Journal of Robust and Nonlinear Control*, vol. 26, no. 11, pp. 2314–2337, 2016.
- [25] B.-Z. Guo and Z.-L. Zhao, "On convergence of the nonlinear active disturbance rejection control for mimo systems," SIAM Journal on Control and Optimization, vol. 51, no. 2, pp. 1727–1757, 2013.
- [26] Z.-L. Zhao and B.-Z. Guo, "A nonlinear extended state observer based on fractional power functions," *Automatica*, vol. 81, pp. 286–296, 2017.
- [27] S. Li, J. Yang, W.-H. Chen, and X. Chen, "Generalized extended state observer based control for systems with mismatched uncertainties," *IEEE Transactions on Industrial Electronics*, vol. 59, no. 12, pp. 4792– 4802, 2012.

- [28] M. Fazlyab, M. Morari, and G. J. Pappas, "Safety verification and robustness analysis of neural networks via quadratic constraints and semidefinite programming," *IEEE Transactions on Automatic Control*, vol. 67, no. 1, pp. 1–15, 2022.
- [29] M. Fazlyab, A. Robey, H. Hassani, M. Morari, and G. Pappas, "Efficient and accurate estimation of lipschitz constants for deep neural networks," in *Advances in Neural Information Processing Systems*, vol. 32, Curran Associates, Inc., 2019.
- [30] R. Y. Zhang and J. Lavaei, "Efficient algorithm for large-and-sparse lmi feasibility problems," in 2018 IEEE Conference on Decision and Control (CDC), pp. 6868–6875, 2018.
- [31] R. Madani, S. Sojoudi, G. Fazelnia, and J. Lavaei, "Finding low-rank solutions of sparse linear matrix inequalities using convex optimization," SIAM Journal on Optimization, vol. 27, no. 2, pp. 725–758, 2017.
- [32] J. T. Bosworth, Linearized aerodynamic and control law models of the X-29A airplane and comparison with flight data, vol. 4356. NASA, 1992
- [33] A. Alleyne, "A comparison of alternative intervention strategies for unintended roadway departure (urd) control," *Vehicle System Dynamics*, vol. 27, no. 3, pp. 157–186, 1997.
- [34] J. P. Gauthier and I. A. K. Kupka, "Observability and observers for nonlinear systems," SIAM Journal on Control and Optimization, vol. 32, no. 4, pp. 975–994, 1994.

# APPENDIX I PROOF OF LEMMA

#### A. Lemma 2

*Proof:* The proof is a direct extension of Lemma 1. Specifically, the left side of above inequality is equivalent to

$$\sum_{k=1}^K \sum_{i=1}^{n_{\sigma_k}} \lambda_{\sigma_k,i} \underbrace{\left(w_{\sigma_k,i} - \alpha_{\sigma_k,i}\xi_{\sigma_k,i}\right) \left(\beta_{\sigma_k,i}\xi_{\sigma_k,i} - w_{\sigma_k,i}\right)}_{\geq 0, \text{ due to } w_{\sigma_k,i} = \sigma(\xi_{\sigma_k,i}) \geq 0.} \geq 0.$$

#### B. Lemma 3

*Proof:* We show that  $Z=D_1+\epsilon D_0\succ O$ , i.e.,  $x^\top Zx>0,\ \forall x\neq 0.$  By the spectral theorem,  $D_1\succ O$  means that  $x^\top D_1x\geq \lambda_{\min}(D_1)\left\|x\right\|_2^2.$  From Cauchy-Schwartz's inequality, we imply that

$$x^{\top}D_0x \ge -|x^{\top}D_0x| \ge -\|D_0\|_2\|x\|_2^2$$
.

Then, it follows that

$$x^{\top}Zx = x^{\top}D_1x + \epsilon x^{\top}D_0x \ge (\lambda_{\min}(D_1) - \epsilon \|D_0\|_2) \|x\|_2^2.$$

Hence, for all 
$$\epsilon \in \left(0, \frac{\lambda_{\min}(D_1)}{\|D_0\|_2}\right)$$
, we have  $x^\top Z x > 0$ , i.e.,  $D_1 + \epsilon D_0 \succ O$ .



Song Chen received the bachelors degree in mathematics from China University of Petroleum, Beijing, China, in 2020. He is currently working toward the Ph.D. degree in operational research and cybernetics with Zhejiang University, Hangzhou, China.

His research interests include nonlinear control, learning-based control, machine learning theory, and their applications in robotics.



**Tehuan Chen** received the bachelors degree from Hangzhou Dianzi University, Hangzhou, China, in 2011, and the Ph.D. degree from the College of Control Science and Engineering, Zhejiang University, Hangzhou, in 2016.

He is currently an Associate Professor with the School of Mechanical Engineering and Mechanics, Ningbo University, Ningbo, China. His research interests include robotics, optimal control, and distributed parameter systems.



**Chao Xu** (Senior Member, IEEE), received the Ph.D. degree in mechanical engineering from Lehigh University, Bethlehem, PA, USA, in 2010.

He is currently Associate Dean and Professor of Controls and Autonomous Systems with the College of Control Science & Engineering, Zhejiang University (ZJU). He serves the inaugural Dean of ZJU Huzhou Institute, as well as plays the role of the Managing Editor for two international journals, e.g., IET Cyber-Systems and Robotics (IET-CSR), and Journal of Indus-

trial and Management Optimization (JIMO). His research expertise is Cybernetic Physics and Autonomous Mobility in general, with a focus on, modeling and control of aerial robotics with applications, machine learning for dynamic systems and control, visual sensing and machine learning for complex fluids.



Jian Chu (Senior Member, IEEE) was born in 1963. He received the B.Sc., M.S., and Ph.D. degrees from Zhejiang University (ZJU), Hangzhou, China, in 1982, 1984, and 1989, respectively. He attended the joint Ph.D. Program of ZJU and Kyoto University, Kyoto, Japan.

After that, he joined the faculty of ZJU, where he became a Full Professor in 1993. He is the Founder of the Institute of Cyber-Systems and Control, ZJU. He is also the Founder of the SUPCON Group, Hangzhou, which is consid-

ered as the top automation company. His current research interests include industrial process automation and computer control systems (i.e., industrial operating systems and control-module-on-chip).